Cenozoic denudation of Corsica in response to Ligurian and Tyrrhenian extension: results from apatite fission-track thermochronology.

Bouchra Zarki-Jakni, Pieter van Der Beek, Gérard Poupeau, Marc Sosson, Erika Labrin, Philippe Rossi, Jean Ferrandini

Cenozoic denudation of Corsica in response to Ligurian and Tyrrhenian extension: results from apatite fission-track thermochronology

Bouchra Zarki-Jakni[1], Peter van der Beek[1*], Gérard Poupeau[1,2], Marc Sosson[3], Erika Labrin[1], Philippe Rossi[4], and Jean Ferrandini[5]

[1] *Laboratoire de Géodynamique des Chaînes Alpines, Université Joseph Fourier, 38041 Grenoble Cedex, France*

[2] now at: *Centre de Recherche en Physique Appliquée à l'Archéologie - Université Bordeaux III, Maison de l'Archéologie, Esplanade des Antilles, 33607 Pessac, France*

[3] *Géosciences Azur, CNRS - Sophia Antipolis, 250 Rue Albert Einstein, 06560 Valbonne, France*

[4] *Bureau de Recherches Géologiques et Minières, Service Géologique National, BP 6009, 45060 Orléans Cedex, France*

[5] *Laboratoire de Géologie, Université de Corte, BP 52, 20250 Corte, France*

Published in: *Tectonics*, Vol. 23, TC1003,
doi: 10.1029/2003TC001535 , 2004

ABSTRACT

The Island of Corsica (France) occupies a unique position in the Western Mediterranean, since it has recorded both the Cenozoic Alpine orogenic history of the area as well as subsequent extensional collapse and oceanic basin formation. We present 41 new apatite fission track (AFT) ages and 23 measurements of track length distributions from Corsica, in order to elucidate its Cenozoic thermal and morphological evolution. AFT ages vary from 10.5±0.8 Ma to 53.8±4.1 Ma and form a clear spatial pattern: oldest ages are encountered in the south-west of the island, with a broad band of ages between 20 and 30 Ma running across the mountainous central area and ages <20 Ma confined to the eastern half of the island. Samples along the western and north-western coasts record km-scale erosional denudation linked to rifting in the Ligurian-Provençal Basin, whereas samples from close to the extensionally inverted Alpine deformation front record a later cooling phase related to Tyrrhenian extension. The eastward-younging pattern of AFT ages suggests the migration of a 'wave' of erosional denudation from west to east across the island, apparently controlled by the migrating locus of extension. Our AFT data therefore support models of Mediterranean extension controlled by slab roll-back.

1. INTRODUCTION

The island of Corsica occupies a central position within the Western Mediterranean, a region characterized by a succession of Cenozoic oceanic basins surrounded by collisional mountain belts (Figure 1). Its geological history is unique in that the island has recorded both the Alpine collisional orogenic evolution of the area as well as the subsequent extensional collapse and basin formation that characterizes the Western Mediterranean. It is therefore particularly well-suited to study the kinematics and dynamics of extension in a general collisional setting [e.g., Jolivet and Faccenna, 2000]. Moreover, the island presents a unique geological framework on a relatively small territory, including well-preserved Hercynian basement rocks as well as alpine metamorphic units.

The island of Corsica is also morphologically exceptional, in that it has by far the highest mean elevation and relief of all Western Mediterranean islands. The origin of the topography surrounding the Western Mediterranean basins, long considered to be a relic of preextensional orogenic events, may in fact be strongly linked to extension, either through flexural or thermal mechanisms [e.g., Cloetingh et al., 1992; Lewis et al., 2000].

Apatite fission-track thermochronology (AFT) has become an invaluable tool to decipher the history of cooling and vertical motions in both orogenic and rifted margin settings [e.g., Gallagher and Brown, 1997; Gallagher et al., 1998] and, in the Corsican case, may provide a unique opportunity to study the thermal, tectonic and morphological response of the upper continental crust to both syn- and post-orogenic extension. Previous AFT studies on Corsica, based on the now outdated population dating method, reported ages between 30 and 45 Ma, pre-dating major extension [Carpéna et al., 1979; Lucazeau and Mailhé, 1986; Mailhé et al., 1986]. More recent ^{40}Ar-^{39}Ar thermochronology in northwestern Corsica [Brunet et al., 2000], however, showed that these ages must be erroneous because they are older than mica ages of 33-25 Ma obtained from rocks from the same region. The mica ages are corroborated by a recent AFT study of northwestern Corsica [Cavazza et al., 2001], which showed AFT ages as young as 14 Ma in this area.

We report 41 new AFT ages, together with 23 measurements of track length distributions, in order to obtain a clearer insight into the late-stage cooling history of Corsica and its relation to Mediterranean extension. Our AFT ages show a clear link between erosional denudation of Corsica and rifting of the Ligurian and Tyrrhenian basins surrounding the island. Moreover, the eastward younging pattern of AFT ages suggests that a 'wave' of denudation traversed the island and was controlled by the migration of the locus of extension. Our data therefore have implications for the dynamics of Western Mediterranean extension and are consistent with models in which this extension is controlled by slab roll-back.

In the following, we first briefly review the geodynamic and geomorphic setting of Corsica. We then present and interpret our data, and discuss the inferences we can draw from it with respect to the tectonic and morphologic response of the island to extension in the basins surrounding it.

2. TECTONIC AND GEOMORPHIC SETTING

2.1. Onshore Geology

The geological history of Corsica is closely linked to that of the western Alps, of which it formed the southward continuation before the opening of the Ligurian-Provençal basin in the Oligocene, and to the Tyrrhenian-Apenninic domain after that time.

The island has traditionally been divided into two structural domains which are profoundly different not only geologically, but in all geographical respects [e.g., Durand Delga, 1978] (Figure 2). The western two-thirds of the island are known as "Hercynian Corsica" and consist mainly of a very large granitic batholith. The northeastern part of the island or "Alpine Corsica", in contrast, is built up of both oceanic and continental thrust sheets that are mainly characterized by late Mesozoic to Cenozoic High-Pressure / Low-Temperature (HP/LT) metamorphism.

Pre-Hercynian remnants are rare in Corsica and are limited to a few occurrences of amphibolite-facies polymetamorphic rocks in the south and northwest of the island. These have yielded both Late Precambrian ("Pan African") and Variscan isotopic ages [Rossi et al., 1995]. Most of Hercynian Corsica is made up of a composite granitoid batholith with intrusion ages between 340 and 260 Ma [Cocherie et al., 1984] that continues southward to form the basement of Sardinia. This Carboniferous batholith is itself overlain and intruded by Permian alkaline and calc-alkaline volcanic and plutonic complexes. The Hercynian basement is cut by major NE-SW oriented, late Hercynian, left-lateral strike-slip faults.

Alpine Corsica consists of a complex nappe-stack of mainly oceanic origin, with intercalated slices of continental basement, which was thrust westwards onto the continental basement of western Corsica (Figure 2; see also Figure 11) [e.g., Durand Delga, 1978; Mattauer et al., 1981]. HP/LT (blueschist and eclogite facies) metamorphism occurs in all but the structurally highest (*i.e.* Balagne and Nebbio units) nappes. From west to east, and from structurally high to lower positions, the most important nappes are the Balagne and Nebbio units, the Tenda Massif and the Corte thrust slices, and the "Schistes Lustrés" nappe [e.g., Brunet et al., 2000, and references therein; Malavieille et al., 1998]. The Balagne and Nebbio units are made up of un-metamorphosed oceanic crust; the westernmost Balagne thrust sheet overlies the Hercynian basement and intervening Eocene foreland basin deposits. The Tenda Massif and the Corte thrust slices consist of pieces of continental basement and their Mesozoic cover, metamorphosed in blueschist facies conditions. The “Schistes Lustrés” nappe is a stack of mainly oceanic units including calcschists, serpentinites, ophiolites and minor continental gneisses. Eclogite facies metamorphism is encountered in the Schistes Lustrés nappe, both within ophiolitic metabasites as well as in the continental gneissic units [Caron, 1994; Caron and Péquignot, 1986; Lahondère, 1996].

The deformation history of Alpine Corsica involves a first phase of top-to-the-west thrusting coeval with the HP/LT metamorphism [Mattauer et al., 1981] . The age of HP/LT metamorphism and compressional deformation remains debated; whereas Malavieille et al. [1998] favor an Eo-Alpine (Mid-Late Cretaceous) age based on scarce isotopic data, Brunet et al. [2000] argue for an Eocene age of peak metamorphism, by comparison with the western Alps in continental France [e.g., Rubatto and Hermann, 2001 and references therein]. During the Oligocene, the sense of shear reversed to penetrative top-to-the-east extension [Daniel et al., 1996; Jolivet et al., 1990]. The contact between the Tenda Massif and the Schistes Lustrés nappes was reactivated as an extensional detachment (the East Tenda shear zone), giving rise to the present-day structural setting of the Tenda Massif inferred to be a metamorphic core complex [Fournier et al., 1991] (cf. Figure 11). Rapid denudation and cooling accompanied the extensional collapse of Alpine Corsica and has been dated at 33-25 Ma by ^{40}Ar-^{39}Ar thermochronology on white micas [Brunet et al., 2000]. The extensional tectonics led to the formation of small extensional basins (e.g. Saint Florent Basin), as well as the much larger Aléria Basin on the eastern coastal plain of Corsica [Fournier et al., 1991]. The latter is a strongly subsiding basin, filled with over 2 km of Neogene sediments, and continuous with the offshore Corsica basin. Sedimentation within these basins started in Burdigalian (~18 Ma) times [Ferrandini et al., 1996; Orzag-Sperber and Pilot, 1976].

2.2 Offshore Extensional Basins

The Ligurian-Provençal basin, which separates the Corsica-Sardinia block from mainland France (Figure 1), started rifting at around 30 Ma, as indicated by syn-rift sediments that occur both onshore and offshore on the northern Ligurian (Provençal) margin [Bellaiche et al., 1976], in the Gulf of Lions [Séranne, 1999] and in the Sardinian rift [Cherchi and Montadert, 1982]. The center of the basin is underlain by thin oceanic crust [Chamot-Rooke et al., 1999; Réhault et al., 1984]; although this crust has not been dated directly, the timing of oceanic spreading is constrained by the 30° counter-clockwise rotation of the Corsica-Sardinia block between 21 and 19-16 Ma [Montigny et al., 1981; Réhault et al., 1984; Vigliotti and Langenheim, 1995]. The basement of the conjugate Provençal margin of the basin is formed by the Paleozoic Maures-Tanneron crystalline massif, unconformably covered by Permian sediments and volcanics as well as a Meso-Cenozoic sedimentary sequence. Both conjugate margins of the basin show a clear segmentation, with alternating narrow and wide margin segments [Rollet et al., 2002]. The pre-rift tectonic structure of the margin (Hercynian basement versus Alpine thrust sheets) appears to strongly control this segmentation [Rollet et al., 2002].

The Tyrrhenian Sea, which separates the Corsica-Sardinia block from the Apennines on the Italian mainland, appears to have opened diachronously from North to South. East of Corsica, rifting started in the northern Tyrrhenian during Burdigalian (~18 Ma) times [Carmignani et al., 1995; Mauffret et al., 1999]. In the southern Tyrrhenian, however, rifting did not start until the Tortonian (~9 Ma) and migrated southeastward with time [Kastens et al., 1988; Spadini et al., 1995]. Two small oceanic domains, which may have opened since ~3.5 Ma, are recognized within the southern Tyrrhenian basin [Kastens et al., 1988].

Models for the development of these and other extensional basins within the overall Mediterranean context of plate convergence have focused on three possible mechanisms: buoyancy forces resulting from orogenic thickening of the Alpine-Apenninic lithosphere [Dewey, 1988]; rollback of the subducting Ionian-Apulian slab [Jolivet and Faccenna, 2000; Malinverno and Ryan, 1986; Royden, 1993]; or break-off and lateral detachment of this slab [Carminati et al., 1998]. Although contributions from buoyancy forces and slab break-off cannot be excluded [Carmignani et al., 1995; Rollet et al., 2002], the overall continuous migration of extension and associated volcanism to the south-east favors a rollback mechanism [Jolivet and Faccenna, 2000]. Such a mechanism for basin opening is also supported by results from both numerical [Bassi et al., 1997] and analog [Facenna et al., 1996] modeling experiments.

2.3 Geomorphology

Corsica is characterized by spectacular relief: although the island has a surface area of less than 9000 km^2, its highest point (Mt. Cinto) culminates at 2710 m, at a distance of only 24 km from the coast and 50 km from the toe of the continental margin. The mean elevation of the island is 565 m, and mean relief (on a 2×2 km scale) is ~150 m. Highest relief (> 600 m) is encountered in the north-west of the island and along the central high-elevation ‘backbone’, adjacent to the Alpine deformation front. Both maximum and mean elevation, as well as mean relief, is significantly higher in Corsica than in any of the other western Mediterranean islands.

The morphology of Hercynian Corsica is distinctly different from that of Alpine Corsica, and mean elevation and relief are significantly higher in the former than in the latter. Hercynian Corsica consists of high-relief mountain massifs, with 20 summits of >2000 m elevation, deeply incised by westward-draining linear gorges (Figure 3) that continue offshore into deep submarine canyons. Overall, the drainage pattern of western Corsica is characteristic of a high-elevation rifted margin with an interior drainage divide and a “gorge-like” escarpment [e.g., Seidl et al., 1996]. The southern and central parts of the island show an asymmetric morphology, with the drainage divide occurring ~10 km east of highest central peaks and corresponding to a steep eastward-facing escarpment adjacent to the eastern Aléria coastal plain (Figure 4b). The asymmetry switches toward the north, however (Figure 4a), where the eastward-draining Golo River and its tributaries have cut back through the Alpine deformation front and deep into the Hercynian massifs. Here the northwest margin is formed by a steep westward facing “drainage-divide” escarpment. The tectonic boundary between Hercynian and Alpine Corsica is morphologically accentuated by the deep longitudinal valleys of the northward-draining Ostriconi River and the middle reach of the east-draining Golo River and its tributaries.

3. APATITE FISSION-TRACK DATA

3.1. Sampling and Procedures

We concentrated our sampling campaign on Hercynian Corsica because the lithologies exposed in this part of the island are much more suitable for fission-track thermochronology than those in Alpine Corsica. We collected 52 samples from the Hercynian granites and gneisses, along three approximately east-west oriented profiles, at elevations between sea level and 1440 m (Figures 3, 4). Another ten samples were collected from the southern third of the island, and sixteen samples from Alpine Corsica (mostly in the northern Cap Corse area) and the contact zone between Hercynian and Alpine Corsica. Of these samples, 41 proved suitable for dating, and we were able to obtain track lengths on 23 of them (Figure 3;

Table 1).

Apatites were recovered from whole-rock samples using standard magnetic and heavy liquid separation techniques, mounted in epoxy, polished and etched in a 1M HNO_3 solution at 20°C for 50 s. All samples were dated by the external detector method, using a zeta calibration factor for Fish Canyon and Durango age standards [Hurford, 1990]. Samples were irradiated at the well-thermalized ORPHEE facility of the *Centre d'Etudes Nucléaires* in Saclay, France, with a nominal fluence of 2.5×10^{15} neutrons/cm^2. Neutron fluences were monitored using CN5 and NBS962 dosimeter glasses. All samples were dated by B. Jakni; 22 measurements were replicated by E. Labrin. All replicate measurements were within 2σ error of each other and all but two within 1σ; the highest-precision measurement of the replicates is reported in Table 1. All length measurements were performed by B. Jakni by digitizing the track ends using a drawing tube. A detailed description of the procedure as well as data for glass standards and zeta calibration values are reported by Jakni [2000].

3.2. Results and Interpretation

Apatite fission-track (AFT) data are summarized in Table 1; all ages are quoted as central ages with $\pm1\sigma$ uncertainties throughout. AFT ages are all Cenozoic and vary from 10.5±0.8 Ma (CO56) to 53.8±4.1 Ma (CO48). All but four samples show very low dispersion (D < 10%, $P(\chi^2) \geq 90\%$), suggesting that chemical heterogeneity of the apatites is not a problem in the crystalline rocks sampled (Figure 5). Mean Confined Track Lengths (MTL) for our samples vary between 12.8±0.2 μm (CO63) and 14.5±0.2 μm (CO12), with standard deviations (SD) between 0.5 and 2.0 μm. Many samples have relatively long MTL (> 13.5 μm) and narrow track-length distributions (SD ≤ 1.5 μm; cf. Figure 7), suggesting relatively rapid cooling from 120°C to surface temperatures.

Most of our AFT ages are significantly younger than the Mesozoic-Eocene ages reported for Corsican samples by Lucazeau and Mailhé [1986] and Mailhé et al. [1986]. The ages reported by these older studies were, however, based on dating by the population method; they are also older than high-temperature ^{40}Ar-^{39}Ar white mica ages on samples from similar areas [Brunet et al., 2000]. We will therefore not consider them further here. Our data are, in contrast, fully compatible with newer data from northwestern Corsica reported by Cavazza et al. [2001] and we will incorporate these data in our discussion below.

There is no clear relationship between sample age and elevation (Figure 6); although some individual groups of samples (e.g., Figure 4a, b) provide consistent age-elevation patterns suggesting denudation rates of 100-400 m/My, there are other groups (e.g., samples from Cap Corse or the Tenda massif) that show negative age-elevation trends.

In contrast to the apparent lack of correlation between sample age and elevation, the geographical spread in ages and track-length distributions shows a very clear pattern (Figure 7). AFT ages ≥ 30 Ma are only encountered in the southwest of the island. The oldest of these samples (CO48, CO59, CO60) have Eocene (> 40 Ma) AFT ages and MTL between 12.7 and 13.5 µm, with MTL increasing with increasing AFT age. Two samples with intermediate ages of 30-35 Ma (CO62, CO63) have low MTL (12.8 – 13.0 µm) and relatively wide track-length distributions (SD = 1.7 – 2.0 µm). AFT ages between 20 and 30 Ma are encountered within a crescent-shaped band running from the northwest coast of the island, between the Gulfs of St. Florent and Ajaccio toward the Gulf of Sta. Manza in the southeast. These samples have MTL between 13.3 and 14.1 µm, with relatively narrow (SD < 1.8 µm) track length distributions. AFT ages younger than 20 Ma are only encountered east of the crescent-shaped band defined above, and AFT ages significantly younger than 15 Ma are concentrated around the Alpine detachment and within Alpine Corsica (Cap Corse region). Samples with AFT ages between 15 and 20 Ma (CO12, CO16, CO27) have MTL > 14 µm and narrow track length distributions. MTL tends to decrease for samples with AFT ages <15 Ma (CO3, CO55, CO69, CO76), which show MTL between 13.5 and 13.8 µm and SD 1.3 – 2.0 µm.

A plot of MTL versus AFT age (Figure 8) also shows a distinct trend in the data: MTL increases with AFT age for samples with ages > 40 Ma, is low for samples with ages between 30-35 Ma, and rises again to form an (ill-defined) peak for samples with AFT ages between 15-23 Ma. This pattern resembles the characteristic 'boomerang' trend of samples exhumed from different depths and paleo-temperatures by a single rapid cooling event [e.g. Gallagher et al., 1998]. Such trends have been described from other rifted margins [e.g., Gallagher and Brown, 1997; Omar et al., 1989] and the MTL peak dating the cooling event was shown to correspond to the age of continental break-up on these margins. In our case, the ages corresponding to the peak in MTL overlap with the timing of oceanic spreading in the Ligurian-Provençal basin (cf. Section 2.2).

In order to explore the Cenozoic cooling history of the regions defined above in more detail, we have used the confined fission track length distribution of selected samples to infer time-temperature paths. We use a genetic algorithm for the inversion [Gallagher, 1995] that is based on the annealing model established for Durango apatite by Laslett et al. [1987]. The relationship between the time-temperature history of a sample and its annealing history as expressed by the track length distribution is dependent on the chemical composition of the apatites analyzed [Carlson et al., 1999; Green et al., 1986], which may vary strongly even for crystalline basement samples [O'Sullivan and Parrish, 1995]. Chemical composition was analyzed for only one sample in the present study; [Cl] / [F] ratios vary between 0 and 0.1 in this sample [Jakni, 2000]. The close clustering of single-grain ages in most of our samples argues against significant chemical variation. As we do not dispose of other compositional data, we refrain from using newer multi-kinetic annealing models [Ketcham et al., 1999]. In our interpretation of the modeled thermal histories, we keep in mind, however, the possible artifacts inherent in the Laslett et al. [1987] parameterization, specifically the apparent underestimation of low-temperature annealing that often leads the model to predict spurious late-stage cooling [e.g., Corrigan, 1993; cf. review by Ketcham et al., 1999].

Figure 9 shows results of the inversion. A sample from the oldest group of ages encountered in SW Corsica (CO62) shows slow and monotonous cooling (≤ 2.5 °C My^{-1}) through the apatite Partial Annealing Zone (PAZ; 60 – 110 °C) between ~40 and ~7 Ma, with an apparent increase in cooling rates during cooling from <60 °C to surface temperatures in the last 7 Ma. However, late Chattian to Burdigalian (~25-18 Ma) sedimentary deposits crop out at several locations in SW Corsica [e.g. Bonifacio Basin, Orzag-Sperber and Pilot, 1976; Vazzio conglomerate, Ferrandini et al., 1999], as well as volcanics dated at ~19 Ma [Ottaviana-Spella et al., 1996]. These deposits clearly show that SW Corsican samples were close to the surface around the Oligocene-Miocene boundary (e.g., ~25-20 Ma). Although the volcanic and sedimentary deposits are obviously erosional remnants, Neogene erosion has probably not been more than a few hundred meters. We therefore prefer to interpret the apparent late cooling event recorded by this and other samples as a model artifact caused by the underestimation of low-temperature annealing in the Laslett et al. [1987] algorithm used.

The thermal history of samples from the 20-25 Ma age group, widely encountered in western and northwestern Corsica (Figure 7) and represented by sample CO36, is radically different from that of older samples. These samples show rapid cooling of up to 9 °C My^{-1} through the apatite PAZ between ~27 and ~18 Ma, coinciding with the time of continental rifting and subsequent oceanic spreading in the Ligurian-Provençal Basin. Again, the inversion predicts a subsequent phase of stability followed by rapid late (<4-7 Ma) cooling to surface temperatures, but we do not consider this part of the predicted cooling history to be reliable.

Samples with AFT ages <20 Ma from the central part of the island and the contact zone between Alpine and Hercynian Corsica (e.g., CO27, CO76), show similar cooling histories as those from the 20-25 Ma age group, with rapid cooling at ~10 °C My^{-1} through the apatite PAZ. The phase of rapid cooling, however, occurs later in these samples; between 18-13 Ma for samples with AFT ages of 15-20 Ma (e.g., CO27) and between 15-8 Ma for samples with AFT ages <15 Ma (e.g., CO76). Rapid cooling within these samples appears to coincide with subsidence and the deposition of thick Burdigalian to Serravalian deposits in the eastern coastal plain and Corsica Basin [Orzag-Sperber and Pilot, 1976] as well as in the smaller Saint-Florent half-graben [Ferrandini et al., 1996].

In order to translate these cooling histories into denudation histories, we need to have an estimate of the thermal gradient. Heat flow data from Corsica have been reported by Lucazeau and Mailhé [1986; see also Della Vedova et al., 1995]. Although heat flow values are relatively high (varying from 76±10 mW m^{-2} for Hercynian Corsica to 81±19 mW m^{-2} for Alpine Corsica), geothermal gradients for Hercynian Corsica are modest (varying from 26 to 31 °C km^{-1}) because of the high thermal conductivity of the Hercynian granites (2.5 – 3.0 W m^{-1} °C^{-1}) [Lucazeau and Mailhé, 1986]. Using these geothermal gradient values and a mean surface temperature of 16°C [e.g., http://www.meteo.fr/temps/monde/climats/station/254.htm], the amount of denudation associated with rapid cooling of the samples CO36, CO27 and CO76 varies between a minimum of 1.9-2.3 km (assuming that samples cooled only to the top of the PAZ at 60 °C during this phase), with subsequent slower denudation of 1.3-1.5 km, and a maximum of 3.4-4.0 km (assuming that samples cooled down to surface temperatures during the rapid cooling phase). Denudation rates associated with the rapid cooling phase are in the order of 290-380 m My^{-1}.

4. DISCUSSION

The AFT ages and track length distributions encountered in Corsica show clear spatial trends that we interpret to reflect cooling and denudation of Corsica in response to extension and subsequent continental break-up in the Ligurian-Provençal and Tyrrhenian basins. Significant cooling and km-scale denudation of Corsica appears to have occurred during Miocene times. In contrast to the crystalline basement massifs of the Alpine and Pyrenean orogens [e.g., Bigot-Cormier et al., 2003; Bogdanoff et al., 2000; Fitzgerald et al., 1999; Seward et al., 1999], however, the Corsican AFT data do not require an important phase of Late Miocene – Pliocene (3-5 Ma) cooling.

The spatial trends in the data can be visualized by plotting AFT ages as a function of distance to the major Ligurian-Provençal and Tyrrhenian extensional domains. Figure 10 shows AFT ages as a function of distance to the Ligurian-Provençal margin (taken as the orthogonal distance between each sample and the limit between extended continental and "transitional" crust as mapped by Rollet et al. [2002]), and as a function of distance to the Alpine detachment. Samples close to the Ligurian-Provençal margin have ages close to the age of Ligurian-Provençal break-up except, intriguingly, for sample CO48 which was collected from closest to the margin and has the oldest AFT age in our dataset. This sample may have been collected from a down-faulted block that suffered little denudation Other AFT ages significantly older than rifting are only encountered at distances >80 km from the margin, although other samples far from the margin have AFT ages close to or younger than break-up. This pattern resembles those reported from other rifted margins around the world [Gallagher and Brown, 1997] but includes additional complexity.

The relationship to Tyrrhenian rifting is demonstrated in the lower plot of Figure 10, which shows an increase in AFT ages with distance from the Alpine detachment. Eastward younging of ^{40}Ar-^{39}Ar ages across the Alpine detachment has been demonstrated by Brunet et al. [2000]; our data confirm this trend but also show that the eastward younging is true at the scale of the whole island, including the Hercynian basement of western Corsica.

The migration of the locus of extension from west to east (that is, from the Liguro-Provençal basin in the Late Oligocene to the Apennines in Quaternary times) has been described previously [e.g., Carmignani et al., 1995; Jolivet and Faccenna, 2000], but whether there was a jump with a time gap between the rifting episodes west and east of Corsica or whether the eastward migration was more continuous has been unclear. Our data suggest that a 'wave' of denudation migrated across the island and continues into the Apennines of mainland Italy, where rapid denudation occurred between 6-4 Ma near the Tyrrhenian coast and at <2 Ma in central Italy [Abbate et al., 1999; Balestrieri et al., 2003]. Such a continuous migration of denudation related to extensional tectonics is compatible with models that relate Mediterranean extension to roll-back of the subducting Ionian-Apulian slab [e.g., Brunet et al., 2000; Jolivet and Faccenna, 2000]. We will discuss the relationship between the thermal and denudation history of Corsica and rifting in the Ligurian and Tyrrhenian domains in more detail below.

4.1. Rifted margin uplift and denudation associated with Ligurian-Provençal rifting

The pattern of AFT ages, which are similar to the age of continental break-up close to the margin with older ages encountered further inland (Figure 10a), is characteristic of rapid denudation of a high-elevation rifted margin in response to surface uplift and / or base-level fall induced by rifting [e.g., Gallagher and Brown, 1997; van der Beek et al., 1995]. Although most of the AFT ages in western and northwestern Corsica are close to the age of break-up, the modeling of track length distributions shows that cooling, presumably caused by erosional denudation, started at the onset of rifting, at around 27 Ma (e.g., CO36, Figure 9). This timing for the onset of rapid rift-related denudation is consistent with results from other basement massifs surrounding the Ligurian-Provençal basin, e.g. the Maures-Tanneron Massif [Morillon, 1997; Jakni, 2000] or the Eastern Pyrenees [Maurel et al., 2002].

An intriguing issue concerns the older fission-track ages in southwestern Corsica. The AFT isochrones cut through the Hercynian structure, suggesting that it had little influence on patterns of denudation at this scale. The age pattern is continuous, however, with samples from northern Sardinia [F. Bigot-Cormier, G. Poupeau, and Ph. Rossi, unpublished data] that also show Paleogene AFT ages.

Lateral variation in AFT ages on rifted margins has been argued to reflect a thermal and denudational response to rift propagation, either continuously or in pulses [e.g., Omar and Steckler, 1995; O'Sullivan et al., 1995]. It has been argued that the Ligurian-Provençal rift propagated from SW to NE [Guieu and Roussel, 1990], which would be in accord with the age pattern observed on Corsica. Within the Maures-Tanneron Massif on the conjugate Provençal margin, however, the trend in AFT ages is opposite, from Miocene (~20-25 Ma) ages in the SW to Mesozoic (> 100 Ma) ages in the NE [Jakni, 2000] and is therefore in contradiction with a simple rift-propagation scenario. Alternatively, the age trend could be related to lateral variations in thermal structure of the upper crust and therefore in the temperature at which the samples resided before Cenozoic denudation. However, the only obvious trend in present-day heat flow across Corsica is from West to East, with lowest heat flow values (~64 mW m^{-2}) recorded west of Ajaccio and highest values (~81 mW m^{-2}) in Alpine Corsica [Lucazeau and Mailhé, 1986]. Variations in thermal structure may therefore be invoked to explain the anomalously old age of sample CO48 from west of Ajaccio, in comparison with the other samples from the southwestern age group, but cannot explain the North-South variation in ages between different age groups.

The inversion of confined track length distributions suggests that the cooling and denudation history of the southwestern samples is profoundly different from that of the other Corsican samples, since the southwestern samples do not record any acceleration in cooling related to rifting. This feature suggests that the southwestern part of Corsica, together with northern Sardinia, reacted differently to rifting than western and northwestern Corsica. Southwestern Corsica and northern Sardinia lie adjacent to the Sardinia rift, an aborted branch of the Ligurian-Provençal rift system that continues northward along the southwestern coast of Corsica [Ferrandini et al., 1999; Rollet et al., 2002; Rossi et al., 1998]. Apparently, this aborted rift caused much less denudation of its flanks than the main branch of the system in which extension reached the stage of continental break-up. Significant differences in the amounts of rift flank denudation between aborted rifts and similarly aged rifted margins have been reported from other systems as well, notably in the East African / Ethiopian rift versus the Red Sea and Gulf of Aden [e.g., Abbate et al., 2002; Foster and Gleadow, 1996; Menzies et al., 1997; Mock et al., 2001].

The lateral variations in age patterns are spatially consistent with the lateral segmentation of the margin as mapped from offshore seismic data [Rollet et al., 2002]. They also clearly demonstrate the asymmetry of the conjugate margins of the Ligurian-Provençal basin: when rotated back to their pre-drift position, the >30 Ma ages in southwestern Corsica lie adjacent to <25 Ma ages in the Maures Massif west of Saint Tropez on the conjugate margin, whereas <25 Ma ages in western and northwestern Corsica lie adjacent to ages >60 Ma in the

Tanneron Massif east of Saint Tropez [Jakni, 2000; Morillon, 1997]. These contrasts in AFT ages across the margin appear to be consistent with lateral variations in margin width, with older AFT ages (and less onshore margin denudation) corresponding to wide margin segments and younger AFT ages (more margin denudation) corresponding to narrow segments. It therefore appears that margin segmentation, which itself is probably caused by the inheritance of major tectonic discontinuities [Rollet et al., 2002] has controlled the denudation history of the onshore parts of both conjugate margins of the Ligurian-Provençal basin.

A remaining question concerns the pre-rift topography of western Corsica, and the associated question of whether rifting in the Ligurian-Provençal basin caused uplift of its margins. To unequivocally demonstrate surface uplift related to rifting requires a marker of pre-rift elevation [e.g., Abbott et al., 1997; Brown, 1991; van der Beek et al., 1994], which is non-existent in the basement rocks of Hercynian Corsica. The oldest sediments encountered are Chattian (syn-rift) in the Ajaccio region [Ferrandini et al., 1999] and Burdigalian (post-rift) in northern and southern Corsica [Ferrandini et al., 1996; Orzag-Sperber and Pilot, 1976]. These shallow marine sediments are located close to sea level, indicating little post-rift vertical motions of the Corsican coastline. In northern Corsica, Eocene shallow marine sediments crop out below the thrust contact of the Balagne Nappe at elevations between sea level and ~700 m (Figure 11), suggesting that the integrated Cenozoic vertical motions due to thrust loading, rift-related uplift and erosional unloading are close to zero in that area.

We can attempt to infer the paleo-elevation and uplift history by combining the fission-track and geomorphic data. The morphology of Hercynian Corsica, characterized by deep gorges incising a high-elevation plateau west of the drainage divide, is characteristic of pre-existing high elevation and a pre-existing inland drainage divide on the margin [Kooi and Beaumont, 1994; van der Beek et al., 2002]. The relatively 'flat' AFT age pattern, with ages close to the age of break-up extending up to the present-day drainage divide (Figure 10a) appears to corroborate this inference, as AFT ages associated with flank uplift and a retreating escarpment would show younging away from the margin [Brown et al., 2002; van der Beek and Braun, 2002]. Significant pre-existing topography can also be inferred from the continuous, although limited, detrital flux from the south that is recorded by Provence platform sediments from mid-Cretaceous to Oligocene times [Guieu and Roussel, 1990].

On the other hand, the along-strike variation in denudation histories that appears consistent with margin segmentation is most easily explained as being caused by differential rift-related vertical motions along the different margin segments. Moreover, we will show below that there is evidence from the sedimentary record of northern and eastern Corsica for Neogene surface uplift of at least some of the central Corsican ranges. Therefore, the quantification of rift-related tectonic surface uplift in Hercynian Corsica remains problematic.

4.2. Tectonic and erosional denudation related to Tyrrhenian extension

The pattern of increasing AFT ages with distance from the Alpine-Hercynian contact zone, which was reactivated as an extensional detachment since Oligocene times [e.g., Brunet et al., 2000; Fournier et al., 1991], clearly demonstrates the influence of Tyrrhenian extension on denudation patterns in Corsica. At first sight, it may be tempting to interpret this pattern as being controlled by tectonic exhumation along the Alpine detachment, the slope in the age – distance plot giving an estimate for the rate of extension [e.g., Foster and John, 1999]. However, the pattern of increasing AFT ages extends well beyond the recognized footwall of the detachment (e.g., the Tenda Massif), suggesting that denudation was not solely tectonic in origin. There are a number of other arguments that favor erosional denudation as the main origin for cooling of the central and eastern Corsican samples. We will develop these below.

The relationships between the tectonic structures and the uplift and exhumation history is clearest in northern Corsica because of the presence of the Saint Florent basin, which acts as a marker of deformation, and because the thermochronologic dataset is most extensive in this area. Figure 11 shows a simplified tectonic map of northern Corsica as well as a southwest-northeast cross-section. Our AFT ages between 15.7±1.4 and 22.3±2.2 Ma from this region are coherent with those of Cavazza et al. [2001], which lie between 13.8±1.6 and 19.2±1.0 Ma. The figure shows that there is no significant jump in thermochronologic ages across the Alpine detachment, for neither high- (^{40}Ar-^{39}Ar) nor low- (AFT) temperature systems. The ^{40}Ar-^{39}Ar ages suggest that both the footwall and the hangingwall of the detachment were exhumed rapidly from ~30 Ma onward, tectonic denudation of the hangingwall probably occurring through penetrative ductile extension [Daniel et al., 1996; Jolivet et al., 1990].

Sample CO18 is a mylonitic gneiss cobble from the central part of the St. Florent Basin fill and has an AFT age of 17.6±2.4 Ma. Its most probable source is the East Tenda shear zone.

This age falls within the stratigraphic age of the basin fill (18-12 Ma; Ferrandini et al. [1996]) and overlaps with AFT ages of 15.4±2.0 – 22.3±2.2 Ma from the eastern Tenda Massif as well as with AFT ages of 17.3±1.1 – 20.9±3.9 Ma from the Nebbio and Schistes Lustrés nappes underlying the basin. This concordance in ages, together with MTL ≥14 μm in samples from the Eastern Tenda Massif (e.g., CO12, CO14) indicates very rapid erosional denudation of both the footwall and hangingwall of the East Tenda shear zone between ~20 – 15 Ma.

Whether the ^{40}Ar-^{39}Ar and AFT ages plotted in Figure 11 represent continuous extensional denudation from ~30-15 Ma or rather two phases of denudation, with an intervening tectonically quiet phase between ~25 and ~18 Ma is not clear at present, in spite of the relatively large thermochronological dataset. In order to solve this question, more data will be required, especially from systems with intermediate closure temperatures (e.g., ^{40}Ar-^{39}Ar on K-feldspar, zircon fission track).

Although an important part of the St. Florent Basin fill has its probable source in the Tenda Massif, volcanic fragments which have the Mt. Cinto Massif as a probable source are also abundant [Ferrandini et al., 1996]. At present, the Mt Cinto massif is drained by the Golo River and its tributary the Asco River (Figure 3), which flow around the south of the Tenda massif and are disconnected from the St. Florent basin. It thus appears that drainage has been diverted by surface uplift of the Tenda Massif postdating 12 Ma. The St. Florent Basin itself is folded into an open syncline (Figure 11); this deformation must also have taken place after 12 Ma.

Our samples from Cap Corse (e.g., CO3, CO4, CO74) have AFT ages between 12.3±2.9 and 13.7±1.3 Ma, consistent with a single sample from Cavazza et al. [2001] dated at 15.7±1.1 Ma. These samples suggest that the eastern seaboard of Corsica may record a relatively young final stage of denudation, post-dating the main phase of denudation more to the west by a few million years. These AFT ages are coherent with the existence of thick Serravalian (14-11 Ma) deposits in the Corsica basin and on the eastern coastal plain [Orzag-Sperber and Pilot, 1976] and suggest that this final phase of cooling and denudation is related to opening of the Tyrrhenian basin. Surface and rock uplift affecting Alpine Corsica at that time is suggested by the folding of Cap Corse into a broad anticline and the cessation of supply of material with a provenance from the Mt. Cinto Massif in the eastern coastal plain [Durand Delga, 1978]. Late deformation and denudation of Alpine Corsica may therefore be related to rift-shoulder uplift associated with Tyrrhenian extension. Geomorphic evidence in the form of uplifted and deformed fluvial terraces [Conchon, 1975; Durand Delga, 1978], as well as geodetic data [Lenôtre et al., 1996], suggest that this uplift is still active. A deep seismic sounding profile across Corsica indicates that the lithosphere thins from ~80 km in the west to no more than 40 km in the east [Bethoux et al., 1999]. The late-stage and present-day uplift of eastern Corsica may therefore be supported thermally and / or dynamically, in a similar manner to that envisaged for the Catalan Coastal Ranges by Lewis et al. [2000].

5. CONCLUSIONS

Our AFT data provide clear evidence for large-scale Neogene cooling and erosional denudation of Corsica, related to rifting in the Ligurian-Provençal and Tyrrhenian basins. In more detail, the model we envisage would have Hercynian Corsica sitting at a pre-existing elevation of at least one kilometer before the onset of rifting in the Liguro-Provençal Basin, with a pre-existing drainage divide close to the present-day divide. This pre-existing topography would have been inherited from the Alpine orogenic phase that saw the overthrusting of the Alpine Nappe pile onto the western Corsican Hercynian basement. Rifting and continental break-up in the Ligurian-Provençal Basin triggered km-scale denudation of western Corsica driven by a major base-level drop, possibly rift-related vertical motions, and the individualization of margin segments. Denudation pathways toward the newly-formed oceanic basin appear to have been much more efficient than toward the aborted Sardinian rift branch.

At the same time (*i.e.* ~30 Ma), extensional tectonic denudation started along the inverted Alpine orogenic front, both within the footwall and the hangingwall, as indicated by ^{40}Ar-^{39}Ar data [Brunet et al., 2000]. The AFT data suggest that from 18-20 Ma onward, surface uplift and erosional denudation affected the Tenda Massif in the footwall of the extensional detachment, its denudational detritus being trapped partly in the hanging-wall Saint Florent Basin. The locus of extension and rift-related uplift migrated further east at ~14-12 Ma, when sedimentation shut down in the Saint Florent Basin while it accelerated in the Corsica Basin and eastern coastal plain. At this time, surface uplift and denudation started to affect Alpine Corsica, leading to uplift and denudation of the Cap Corse area and the diversion of large eastward-draining rivers.

The eastward-younging pattern of AFT ages suggests the migration of a ‘wave’ of denudation from west to east across the island, which appears controlled by a continuously migrating locus of extension. Our data therefore support models of Mediterranean extension controlled by slab roll-back.

Acknowledgements

Funding for this project was provided by the *Bureau de Recherches Géologiques et Minières* (BRGM) and the *Institut National des Sciences de l’Univers* under the *Idyl-Extension* and *Géosciences Marines* programmes. We thank Laurent Jolivet and Marc Jolivet, as well as associate editor Marc Daignières, for constructive reviews.

REFERENCES

Abbate, E., M.L. Balestrieri, G. Bigazzi, B. Ventura, M. Zattin, and G.G. Zuffa, An extensive apatite fission-track study throughout the Northern Apennines nappe belt, *Nucl. Tracks Rad. Meas., 31*, 673-676, 1999.

Abbate, E., M.L. Balestrieri, and G. Bigazzi, Morphostructural development of the Eritrean rift flanks (southern Red Sea) inferred from apatite fission track analysis, *J. Geophys. Res., 107*, 2319, doi: 10.1029/2001JB001009, 2002.

Abbott, L.D., E.A. Silver, R.S. Anderson, R. Smith, J.C. Ingle, S.A. King, D. Haig, E. Small, J. Galewski, and W. Sliter, Measurement of tectonic surface uplift rate in a young collisional orogen, *Nature, 385*, 501-507, 1997.

Balestrieri, M.L., M. Bernet, M.T. Brandon, V. Picotti, P. Reiners, and M. Zattin, Pliocene and Pleistocene exhumation and uplift of two key areas of the Northern Apennines, *Quat. Int., 101-102*, 67-73, 2003.

Bassi, G., R. Sabadini, and S. Rebaï, Modern tectonic regime in the Tyrrhenian area: observations and models, *Geophys. J. Int., 129*, 330-346, 1997.

Bellaiche, G., F. Irr, and M. Labarbarie, Découverte de sédiments marins fini oligocène-aquitanien au large du Massif des Maures (Canyon des Stoechades), *C. R. Acad. Sci. Paris, 283*, 319-322, 1976.

Bethoux, N., A. Deschamps, G. Nolet, E. Bertrand, I. Construcci, M. Sosson, and J. Ferrandini, The deep structure of Corsica as inferred by a broadband seismological profile, *Geophys. Res. Lett., 26*, 2661-2664, 1999.

Bigot-Cormier, F., G. Poupeau, and M. Sosson, The denudation history of the Argentera Alpine external crystalline Massif (France-Italy): An overview from the analysis of fission tracks in apatites and zircons, *Tectonophysics, in press*, 2003.

Bogdanoff, S., A. Michard, M. Mansour, and G. Poupeau, Apatite fission track analysis in the Argentera massif: evidence of contrasting denudation rates in the External Crystalline Massifs of the Western Alps, *Terra Nova, 12*, 117-125, 2000.

Brown, R.W., Backstacking apatite fission-track "stratigraphy": A method for resolving the erosional and isostatic rebound components of tectonic uplift histories, *Geology, 19*, 74-77, 1991.

Brown, R.W., M.A. Summerfield, and A.J.W. Gleadow, Denudational history along a transect across the eastern margin (Drakensberg Escarpment) of southern Africa derived from apatite fission-track thermochronology, *J. Geophys. Res., 107*, 2350, doi: 10.1029/2001JB000745, 2002.

Brunet, C., P. Monié, L. Jolivet, and J.-P. Cadet, Migration of compression and extension in the Tyrrhenian Sea, insights from $^{40}Ar/^{39}Ar$ ages on micas along a transect from Corsica to Tuscany, *Tectonophysics, 321*, 127-155, 2000.

Carlson, W.D., R.A. Donelick, and R.A. Ketcham, Variability of apatite fission-track annealing kinetics: I. Experimental results, *Am. Mineral., 84*, 1213-1223, 1999.

Carmignani, L., F.A. Decandia, L. Disperati, P.L. Fantozzi, A. Lazzarotto, D. Liotta, and G. Oggiano, Relationships between the Tertiary structural evolution of the Sardinia-Corsica-Provençal Domain and the Northern Apennines, *Terra Nova, 7*, 128-137, 1995.

Carminati, E., M.J.R. Wortel, W. Spakman, and R. Sabadini, The role of slab detachment processes in the opening of the western-central Mediterranean basins: some geological and geophysical evidence, *Earth Planet. Sci. Lett., 160*, 651-665, 1998.

Caron, J.M., Metamorphism and deformation in Alpine Corsica, *Schweiz. Mineral. Petrogr. Mitt., 74*, 105-114, 1994.

Caron, J.M., and G. Péquignot, The transition between blueschist and lawsonite-bearing eclogites based on observations from Corsican metabasalts, *Lithos, 19*, 205-218, 1986.
Carpéna, J., D. Mailhé, C.W. Naeser, and G. Poupeau, Datation d'une phase éocène en Corse, *C.R. Acad. Sci. Paris, 289*, 829-832, 1979.
Cavazza, W., M. Zattin, B. Ventura, and G.G. Zuffa, Apatite fission-track analysis of Neogene exhumation in northern Corsica (France), *Terra Nova, 13*, 51-57, 2001.
Chamot-Rooke, N., J.M. Gaulier, and F. Jestin, Constraints on Moho depth and crustal thickness in the Liguro-Provençal basin from 3D gravity inversion: Geodynamic implications, in *The Mediterranean Basins: Tertiary Extension within the Alpine Orogen*, edited by B. Durand, L. Jolivet, F. Horvàth and M. Séranne, Geol. Soc. Spec. Publ., vol. 156, pp. 37-62, 1999.
Cherchi, A., and L. Montadert, Oligo-Miocene rift of Sardinia and the early history of the western Mediterranean basin, *Nature, 298*, 736-739, 1982.
Cloetingh, S., P.A. van der Beek, D. van Rees, T.B. Roep, C. Biermann, and R.A. Stephenson, Flexural interaction and the dynamics of Neogene extensional basin formation in the Alboran-Betic region, *Geo-Marine Letters, 12*, 66-75, 1992.
Cocherie, A., P. Rossi, and L. Le Bel, The variscan calc-alkalic plutonism of Western Corsica: Mineralogy and major and trace element geochemistry, *Phys. Earth Planet. Int., 35*, 145-178, 1984.
Conchon, O., Les formations quaternaires de type continental en Corse orientale, PhD thesis, 514 pp., Université Paris VI, 1975.
Corrigan, J., Apatite fission-track analysis of Oligocene strata in South Texas, U.S.A.: Testing annealing models, *Chem. Geol. (Isot. Geosci. Sect.), 104*, 227-249, 1993.
Daniel, J.M., L. Jolivet, B. Goffé, and C. Poinssot, Crustal-scale strain partitioning: footwall deformation below the Alpine Oligo-Miocene detachment of Corsica, *J. Struct. Geol., 18*, 41-59, 1996.
Della Vedova, B., F. Lucazeau, V. Pasquale, G. Pellis, and M. Verdoya, Heat flow in the tectonic provinces crossed by the southern segment of the European Geotraverse, *Tectonophysics, 244*, 57-74, 1995.
Dewey, J.F., Extensional collapse of orogens, *Tectonics, 7*, 1123-1139, 1988.
Durand Delga, M. (ed.), *Corse; Guide Géologique Régional*, 208 pp., Masson, Paris, 1978.
Faccenna, C., P. Davy, J.P. Brun, R. Funiciello, D. Giardini, M. Mattei, and T. Nalpas, The dynamics of back-arc extension: An experimental approach to the opening of the Tyrrhenian Sea, *Geophys. J. Int., 126*, 781-795, 1996.
Ferrandini, M., J. Ferrandini, M.D. Loyë-Pilot, J. Butterlin, J. Cravatte, and M.C. Janin, Le Miocène du bassin de Saint Florent (Corse): modalités de la transgression du Burdigalien supérieur et mise en évidence du Serravalien, *GeoBios, 31*, 125-137, 1996.
Ferrandini, J., P. Rossi, M. Ferrandini, G. Farjanel, L. Ginsburg, M. Schuler, and F. Geissert, La formation conglomératique du Vazzio près d'Ajaccio (Corse-du-Sud), un témoin des dépôts du Chattien supérieur continental synrift en Méditerranée occidentale, *C.R. Acad. Sci. Paris, 329*, 271-278, 1999.
Fitzgerald, P.G., J.A. Muñoz, P.J. Coney, and S.L. Baldwin, Asymmetric exhumation across the Pyrenean orogen: implications for the tectonic evolution of a collisional orogen, *Earth Planet. Sci. Lett., 173*, 157-170, 1999.
Foster, D.A., and A.J.W. Gleadow, Structural framework and denudation history of the flanks of the Kenya and Anza Rifts, East Africa, *Tectonics, 15*, 258-271, 1996.
Foster, D.A., and B.E. John, Quantifying tectonic exhumation in an extensional orogen with thermochronology: examples from the southern Basin and Range Province, in *Exhumation Processes: normal faulting, ductile flow, and erosion*, edited by U. Ring,

M. Brandon, G.S. Lister and S.D. Willett, Geol. Soc. Spec. Publ., vol. 154, pp. 356-378, 1999.
Fournier, M., L. Jolivet, B. Goffé, and R. Dubois, Alpine Corsica metamorphic core complex, *Tectonics, 10*, 1173-1186, 1991.
Galbraith, R.F., and G.M. Laslett, Statistical models for mixed fission track ages, *Nucl. Tracks Radiat. Meas., 21*, 459-470, 1993.
Gallagher, K., Evolving temperature histories from apatite fission track data, *Earth Planet. Sci. Lett., 136*, 421-435, 1995.
Gallagher, K., and R.W. Brown, The onshore record of passive margin evolution, *J. Geol. Soc. London, 154*, 451-457, 1997.
Gallagher, K., R. Brown, and C. Johnson, Fission track analysis and its applications to geological problems, *Ann. Rev. Earth Planet. Sci., 26*, 519-572, 1998.
Green, P.F., I.R. Duddy, A.J.W. Gleadow, P.R. Tingate, and G.M. Laslett, Thermal annealing of fission tracks in apatite 1. A qualitative description, *Chem. Geol. (Isot. Geosci. Sect.), 59*, 237-253, 1986.
Gueguen, E., C. Doglioni, and M. Fernandez, Lithospheric boudinage in the Western Mediterranean back-arc basin, *Terra Nova, 9*, 184-187, 1997.
Guieu, G., and J. Roussel, Arguments for the pre-rift uplift and rift propagation in the ligurian-provençal basin (NW Mediterranean) in the light of pyrenean-provençal orogeny, *Tectonics, 9*, 1113-1142, 1990.
Hurford, A.J., International union of geological sciences subcommission on geochronology recommendation for the standardization of fission track dating calibration and data reporting, *Nucl. Tracks Radiat. Meas., 17*, 233-236, 1990.
Jakni, B., Thermochronologie par traces de fission des marges conjuguées du bassin liguro-provençal: la Corse et le massif des Maures-Tanneron, PhD. thesis, 344 pp., Université Joseph Fourier, Grenoble, 2000.
Jolivet, L., R. Dubois, M. Fournier, B. Goffé, A. Michard, and C. Jourdan, Ductile extension in Alpine Corsica, *Geology, 18*, 1007-1010, 1990.
Jolivet, L., and C. Faccenna, Mediterranean extension and the Africa-Eurasia collision, *Tectonics, 19*, 1095-1106, 2000.
Kastens, K., J. Mascle, C. Auroux, E. Bonatti, C. Broglia, J. Channell, P. Curzi, K.-C. Emeis, G. Glaçon, S. Hasegawa, W. Hieke, G. Mascle, F. McCoy, J. McKenzie, J. Mendelson, C. Müller, J.-P. Réhault, A. Robertson, R. Sartori, R. Sprovieri, and M. Torii, ODP Leg 107 in the Tyrrhenian Sea: Insights into passive margin and back-arc basin evolution, *Geol. Soc. Am. Bull., 100*, 1140-1156, 1988.
Ketcham, R.A., R.A. Donelick, and W.D. Carlson, Variability of apatite fission-track annealing kinetics: III. Extrapolation to geological time scales, *Am. Mineral., 84*, 1235-1255, 1999.
Kooi, H., and C. Beaumont, Escarpment evolution on high-elevation rifted margins; insights derived from a surface processes model that combines diffusion, advection and reaction, *J. Geophys. Res., 99*, 12191-12210, 1994.
Lahondère, D., Les schistes bleus et les éclogites à lawsonite des unités continentales et océaniques de la Corse alpine, PhD. thesis, 285 pp., Université de Montpellier II, 1996.
Laslett, G.M., P.F. Green, I.R. Duddy, and A.J.W. Gleadow, Thermal annealing of fission tracks in apatite 2. A quantitative analysis, *Chem. Geol. (Isot. Geosci. Sect.), 65*, 1-13, 1987.
Lenôtre, N., J. Ferrandini, M. Delfau, and J. Panighi, Mouvements verticaux actuels de la Corse (France) par comparaison de nivellements, *C.R. Acad. Sci. Paris, 323*, 957-964, 1996.

Lewis, C.J., J. Vergés, and M. Marzo, High mountains in a zone of extended crust: Insights into the Neogene-Quaternary topographic development of northeastern Iberia, *Tectonics, 19*, 86-102, 2000.
Lucazeau, F., and D. Mailhé, Heat flow, heat production and fission track data from the Hercynian basement around the Procençal Basin (western Mediterranean), *Tectonophysics, 128*, 335-356, 1986.
Mailhé, D., F. Lucazeau, and G. Vasseur, Uplift history of thrust belts: An approach based on fission track data and thermal modelization, *Tectonophysics, 124*, 177-191, 1986.
Malavieille, J., A. Chemenda, and C. Larroque, Evolutionary model for Alpine Corsica: mechanism for ophiolite emplacement and exhumation of high-pressure rocks, *Terra Nova, 10*, 317-322, 1998.
Malinverno, A., and W. Ryan, Extension in the Tyrrhenian Sea and shortening in the Apennines as result of arc migration driven by sinking of the lithosphere, *Tectonics, 5*, 227-245, 1986.
Mattauer, M., M. Faure, and J. Malavieille, Transverse lineation and large scale structures related to Alpine obduction in Corsica, *J. Struct. Geol., 3*, 401-409, 1981.
Mauffret, A., I. Construcci, and C. Brunet, Structural evolution of the Northern Tyrrhenian Sea from new seismic data, *Mar. Petrol. Geol., 16*, 381-407, 1999.
Maurel, O., M. Brunel, and P. Monié, Exhumation cénozoïque des massifs du Canigou et de Mont-Louis (Pyrénées orientales, France), *C.R. Geoscience, 334*, 941-948, 2002
Menzies, M., K. Gallagher, A. Yelland, and A.J. Hurford, Volcanic and nonvolcanic rifted margins of the Red Sea and Gulf of Aden: Crustal cooling and margin evolution in Yemen, *Geochim. Cosmochim. Acta, 61*, 2511-2527, 1997.
Mock, C., K. Gallagher, and A. Carter, First apatite fission track study on Pan-African basement in Ethiopia: Preliminary results, in *Proc. European Union of Gesciences XI, J. Conf. Abstr.*, pp. 714, 2001.
Montigny, R., J.B. Edel, and R. Thuizat, Oligo-Miocene rotation of Sardinia: K-Ar ages and paleomagnetic data of Tertiary volcanics, *Earth Planet. Sci. Lett., 54*, 261-271, 1981.
Morillon, A.C., Etude thermo-chronométrique appliquée aux exhumations en contexte orogénique: le Massif des Maures (France) et les Cordillères Bétiques (Espagne), PhD. thesis, 303 pp., Université de Nice, 1997.
Omar, G.I., and M.S. Steckler, Fission track evidence on the initial rifting of the Red Sea: Two pulses, no propagation, *Science, 270*, 1341-1344, 1995.
Omar, G.I., M.S. Steckler, W.R. Buck, and B.P. Kohn, Fission-track analysis of basement apatites at the western margin of the Gulf of Suez rift, Egypt: evidence for synchroneity of uplift and subsidence, *Earth Planet. Sci. Lett., 94*, 316-328, 1989.
Orzag-Sperber, F., and M.D. Pilot, Grands traits du Néogène de Corse, *Bull. Soc. Géol. France, 18*, 1183-1187, 1976.
O'Sullivan, P.B., D.A. Foster, B.P. Kohn, A.J.W. Gleadow, and A. Raza, Constraints on the dynamics of rifting and denudation on the eastern margin of Australia: Fission track evidence for two discrete causes of rock cooling, in *Proc. Pacific Rim Conference*, pp. 441-446, Auckland, New Zealand, 1995.
O'Sullivan, P.B., and R.R. Parrish, The importance of apatite composition and single grain ages when interpreting fission track data from plutonic rocks: a case study from the Coast Ranges, British Columbia, *Earth Planet. Sci. Lett., 132*, 213-224, 1995.
Ottaviana-Spella, M.-M., M. Girard, and A. Cheilletz, Les ignimbrites burdigaliennes du Sud de la Corse. Pétrologie et datations K-Ar, *C.R. Acad. Sci. Paris, 323*, 771-778, 1996.
Réhault, J.-P., G. Boillot, and A. Mauffret, The western Mediterranean basin geological evolution, *Mar. Geol., 55*, 447-477, 1984.

Rollet, N., J. Déverchère, M.-O. Beslier, P. Guennoc, J.-P. Réhault, M. Sosson, and C. Truffert, Back arc extension, tectonic inheritance, and volcanism in the Ligurian Sea, Western Mediterranean, *Tectonics, 21*, 10.1029/2001TC900027, 2002.

Rossi, P., A. Cocherie, and M. Durand-Delga, Arguments géochronologiques en faveur de la présence d'un socle panafrican (cadomien) en Corse, conséquences sur la paléogéographie de l'orogène varisque sud-européen, *C.R. Acad. Sci. Paris, 321*, 983-992, 1995.

Rossi, P., P. Guennoc, J.-P. Réhault, N. Arnaud, B. Jakni, G. Poupeau, M. Tegyey, J. Ferrandini, M. Sosson, M.-O. Beslier, N. Rollet, and R. Gloaguen, Importance du volcanisme calco-alcalin miocène sur la marge sud-ouest de la Corse (campagne MARCO), *C.R. Acad. Sci. Paris, 327*, 369-378, 1998.

Rossi, P., J.C. Lahondère, D. Lluch, M.D. Loye-Pilot, and M. Jaquet, Carte Géologique de France 1:50.000; feuille Saint Florent (1103). Notice explicative, BRGM, Orléans, 1994.

Royden, L.H., Evolution of retreating subduction boundaries formed during continental collision, *Tectonics, 12*, 629-638, 1993.

Rubatto, D., and J. Hermann, Exhumation as fast as subduction?, *Geology, 29*, 3-6, 2001.

Seidl, M.A., J.K. Weissel, and L.F. Pratson, The kinematics and pattern of escarpment retreat across the rifted continental margin of SE Australia, *Basin Res., 8*, 301-316, 1996.

Séranne, M., The Gulf of Lions continental margin (NW Mediterranean) revisited by IBS: an overview, in *The Mediterranean Basins: Tertiary Extension within the Alpine Orogen*, edited by B. Durand, L. Jolivet, F. Horvàth and M. Séranne, Geol. Soc. Spec. Publ., vol. 156, pp. 15-37, 1999.

Seward, D., M. Ford, J. Bürgisser, H. Lickorish, E.A. Williams, and L.D. Meckel III, Preliminary results of fission-track analyses in the southern Pelvoux area, SE France, in *Proc. 3rd Workshop on Alpine Geological Studies*, Biella-Oropa September 29 - October 1, 1997, edited by G. Gosso, F. Jadoul, M. Sella and M.I. Spalla, *Mem. Sci. Geol.*, vol. 51, pp. 25-31, 1999.

Spadini, G., G. Bertotti, and S. Cloetingh, Tectono-stratigraphic modelling of the Sardinian margin of the Tyrrhenian Sea, *Tectonophysics, 252*, 269-284, 1995.

van der Beek, P.A., P.A.M. Andriessen, and S. Cloetingh, Morpho-tectonic evolution of rifted continental margins: Inferences from a coupled tectonic-surface processes model and fission-track thermochronology, *Tectonics*, *14*, 406-421, 1995.

van der Beek, P.A., and J. Braun, Relief development, thermal structure of the crust, and the interpretation of thermochronologic data from rifted margins and mountain massifs, in *International workshop on fission track analysis: Theory and applications*, El Puerto de Santa María (Cádiz), edited by L. Barbero and F. Colombo, *Geotemas*, vol. 4, pp. 161-163, 2002.

van der Beek, P.A., S. Cloetingh, and P.A.M. Andriessen, Mechanisms of extensional basin formation and vertical motions at rift flanks: Constraints from tectonic modelling and fission-track thermochronology, *Earth Planet. Sci. Lett., 121*, 417-433, 1994.

van der Beek, P.A., M.A. Summerfield, J. Braun, R.W. Brown, and A. Fleming, Modeling post-break-up landscape development and denudational history across the southeast African (Drakensberg Escarpment) margin, *J. Geophys. Res., 107*, 2351, doi: 10.1029/2001JB000744, 2002.

Vigliotti, L., and V.E. Langenheim, When did Sardinia stop rotating? New paleomagnetic results, *Terra Nova, 7*, 424-435, 1995.

FIGURE CAPTIONS

Figure 1. A) Tectonic setting of Corsica within the western Mediterranean, showing tectonic elements that were active during the Neogene. Abbreviations: Ba: Balearic islands; C: Corsica; MT: Maures - Tanneron Massif; Sa: Sardinia; Si: Sicily. Modified from Rollet et al. [2002] and Jolivet and Faccenna [2000]. B) Schematic crustal-scale cross-sections across the Ligurian-Provençal Basin, Corsica, the Northern Tyrrhenian Basin and the Apennines (trace of cross sections indicated in A). Compiled and modified from Carmignani et al. [2000], Gueguen et al. [1997], Brunet et al. [2000] and Rollet et al. [2002].

Figure 2. Simplified tectonic map of Corsica, showing locations referred to in text. *V*: Vazzio conglomerate. Box shows location of more detailed map in Figure 11.

Figure 3. 75-m resolution Digital Terrain Model of Corsica, showing sample locations as well as main river valleys referred to in text. Eastings / Northings refer to the *Institut Géographique National* Lambert-IV grid for Corsica. Dashed white line delineates the drainage divide between basins that drain to the Ligurian and Tyrrhenian seas, respectively.

Figure 4. Maximum, mean and minimum elevations along two 20-km wide swaths across (a) northern and (b) central Corsica. AFT ages for samples lying within swaths are indicated. Inset shows location of swaths, as well as location of structural cross-section shown in Figure 11. Half arrows indicate position of Alpine detachment.

Figure 5. Radial plots for representative samples from each of the age groups defined in Figure 7.

Figure 6. Relationship between fission-track age and sample elevation. Note that the three Eocene-age samples (CO48, CO59, CO60) are not included in this plot to avoid clutter; all three of these samples were collected close to sea level.

Figure 7. Distribution of AFT ages and representative horizontal confined track length distributions. Thin line with teeth represents Alpine deformation front (detachment). Names of large gulfs quoted in text are given in italics.

Figure 8. Plot of apatite fission-track age versus mean confined track length for all samples for which track length data were collected in this study. Note that vertical error bars represent standard deviation of track-length distribution rather than formal error on mean track length.

Figure 9. Time-temperature histories of selected samples calculated by inversion of track-length distributions. The shaded lines in the Time / Temperature plots represent solutions that statistically fit the observed data (sample age and track-length distribution); black line is overall 'best-fit' solution for the sample. Note varying timescales in these plots. Top and base of apatite Partial Annealing Zone (PAZ; 60 – 110 °C), within which the thermal histories are well resolved, are shown as dashed horizontal lines. Monte Carlo boxes, within which tie points of Time / temperature histories are constrained to lie, are indicated in dark shading. Upper panels for each plot compare the observed track-length

distribution (shown as histogram) with the predicted probability density function (shown as thick line). $P(\chi^2)$ is the Chi-square probability that the observed and predicted track-length distributions (for the best-fit solution) are similar. Other notations as in Table 1, except N = number of track lengths measured.

Figure 10. AFT ages as a function of distance from the margin (upper plot) and distance from the Alpine detachment (lower plot). Distance from margin is calculated as orthogonal distance between sample and the limit between thinned continental and "transitional" crust as mapped by Rollet et al. [2002] Note inverted x-axis for lower plot so that both profiles are aligned from West (left) to East (right); negative distances in lower plot are for samples from Alpine Corsica (east of the detachment).

Figure 11. Structural map and cross-section of Northern Corsica, showing relationships between the main tectonic units, and their relationship with thermochronologic ages. White arrows indicate Neogene extensional kinematic indicators measured by Daniel et al. [1996], Fournier et al. [1991], and Malavieille et al. [1998] Roman typeset numbers represent AFT ages (bold: this study; plain: from Cavazza et al [2001]), italic numbers are mica Ar-Ar ages from Brunet et al. [2000]. Map and cross section modified from Malavieille et al. [1998] and Rossi et al. [1994].

Table 1. Apatite Fission Track Data From Corsica

Sample	Grid Reference		Altitude (m)	N	ρ_s (N_s) (10^6 cm^{-2})	ρ_i (N_i) (10^6 cm^{-2})	ρ_d (N_d) (10^6 cm^{-2})	P(χ^2) (%)	D (%)	Age ± 1σ (Ma)	MTL ± 1σ (μm)	SD (μm)	No lengths
CO3	576100	265000	370	4	0.106 (23)	0.517 (112)	0.351 (16696)	98	3	12.3±2.9	13.5±1.0	2.0	4
CO4	576060	280450	160	11	0.114 (103)	0.562 (509)	0.416 (16507)	97.5	4	13.7±1.3			
CO5	554850	261550	70	18	0.134 (155)	0.440 (508)	0.390 (7741)	>99.5	4	20.3±2.0			
CO7	559300	262650	330	22	0.155 (191)	0.479 (590)	0.390 (7741)	>99.5	4	21.6±2.1			
CO12[§]	564350	264100	290	20	0.155 (186)	0.652 (782)	0.390 (7741)	>99.5	7	15.7±1.4	14.5±0.2	1.3	39
CO13[§]	567400	263000	218	22	0.167 (220)	0.652 (857)	0.416 (16507)	>99.5	6	18.1±1.5			
CO14[§]	568550	264100	170	38	0.069 (153)	0.205 (453)	0.390 (7741)	>99.5	2.5	22.3±2.2	14.0±0.2	1.3	43
CO16	573750	273150	32	5	0.125 (47)	0.399 (150)	0.390 (7741)	14	16	20.9±3.9	14.2±0.2	1.4	60
CO18	572820	271650	30	9	0.148 (90)	0.598 (346)	0.390 (7741)	98	7	17.6±2.4			
CO22	555900	241200	340	12	0.098 (66)	0.656 (444)	0.746 (17265)	99	8	16.5±2.5			
CO25	551950	239750	459	15	0.125 (156)	0.540 (677)	0.416 (16507)	98	9	16.4±1.6	13.9±0.2	1.1	30
CO26	550100	238750	670	5	0.081 (24)	0.272 (81)	0.351 (16696)	93	6	17.7±4.4			
CO27	549850	238550	677	14	0.465 (431)	2.090 (1938)	0.416 (16507)	38	12	15.8±1.2	14.1±0.1	1.0	82
CO28	548350	238100	755	14	0.128 (95)	0.971 (720)	0.746 (17265)	>99.5	8	14.9±1.9			
CO31	541850	233300	1440	5	0.170 (31)	0.848 (155)	0.746 (17265)	>99.5	1	22.5±4.8			
CO35	564200	243600	250	7	0.104 (32)	0.760 (234)	0.746 (17265)	>99.5	3	15.4±3.3			
CO36[§]	547900	260450	30	20	0.781 (869)	2.042 (2274)	0.351 (16696)	91	9	22.5±1.2	14.1±0.1	1.3	129
CO42[§]	530700	214930	547	20	0.277 (322)	0.742 (862)	0.348 (11034)	98	9	22.0±1.7	14.0±0.1	1.5	120
CO43	530350	215800	550	15	0.211 (253)	0.565 (679)	0.348 (11034)	88	10	22.1±2.0	13.9±0.2	0.5	39
CO44[§]	532250	215200	770	20	0.280 (335)	0.729 (874)	0.348 (11034)	>99.5	7	22.6±1.7	13.4±0.2	1.8	77
CO48[§]	524000	175200	1	21	0.386 (438)	0.422 (479)	0.348 (11034)	>99.5	6	53.8±4.1	13.5±0.3	2.1	47
CO50[§]	536950	192250	612	20	0.199 (284)	0.479 (685)	0.348 (11034)	>99.5	6	24.4±2.0	13.5±0.2	1.5	87
CO51[§]	543350	196630	885	18	0.249 (271)	0.749 (816)	0.348 (11034)	78	11	19.4±1.6			
CO52	560000	201820	1102	19	0.192 (245)	0.857 (1094)	0.416 (16507)	>99.5	5	15.9±1.3	13.5±0.4	2.1	24
CO54	581650	175650	75	16	0.201 (211)	0.697 (732)	0.359 (11388)	98	9	15.6±1.5			
CO55[§]	581700	175700	75	20	0.055 (319)	0.218 (1257)	0.359 (11388)	96	9	12.9±1.0	13.7±0.2	1.5	62
CO56	580850	179800	320	22	0.233 (366)	1.210 (1859)	0.359 (11388)	>99.5	7	10.5±0.8	14.1±0.1	1.4	106
CO58[§]	579700	151300	85	20	0.281 (342)	0.568 (691)	0.359 (11388)	99	8	25.2±1.9	13.3±0.7	2.2	11
CO59	573460	119800	5	20	0.476 (685)	0.553 (795)	0.359 (11388)	>99.5	7	46.7±3.6	12.7±0.2	1.9	93
CO60	561500	132650	70	18	0.616 (886)	0.648 (933)	0.359 (11388)	69	10	51.7±3.8	12.9±0.4	1.9	22
CO61	551750	133200	150	12	0.369 (221)	0.359 (395)	0.359 (11388)	91	9	30.1±3.2			
CO62	550150	142200	280	6	0.393 (173)	0.620 (273)	0.359 (11388)	80	7	34.2±4.2	13.0±0.1	1.7	204
CO63[§]	548600	150350	10	20	0.686 (960)	1.156 (1618)	0.359 (11388)	26	12	29.8±1.7	12.8±0.2	2.0	139

Table 1. (Continued)

Sample	Grid Reference		Altitude (m)	N	ρ_s (N_s) $\times10^6$	ρ_i (N_i) $\times10^6$	ρ_d (N_d) $\times10^6$	$P(\chi^2)$ (%)	D (%)	Age ± 1σ (Ma)	MTL ± 1σ (μm)	SD (μm)	No lengths
CO65	550950	166800	260	21	0.277 (452)	0.727 (1186)	0.359 (11388)	99	8	20.6±1.6	13.4±0.3	1.5	35
CO67	537550	179300	20	20	0.171 (283)	0.453 (752)	0.359 (11388)	95	9	20.4±1.8			
CO69	564800	209380	900	13	0.174 (114)	0.756 (494)	0.336 (8876)	50	14	11.9±1.4	13.8±0.2	1.4	53
CO74	572050	300450	180	10	0.270 (180)	1.054 (703)	0.336 (8876)	>99.5	4	13.0±1.4			
CO76	564400	214650	510	20	0.568 (764)	2.435 (3273)	0.345 (10938)	86	9	12.1±0.8	13.5±0.1	1.3	119
CO79	569650	201300	550	18	0.494 (323)	1.840 (1202)	0.345 (10938)	98	9	14.0±1.2			
CO80	572400	202300	400	11	0.113 (69)	0.799 (487)	0.746 (17265)	>99.5	4	16.0±2.3			
CO81	573200	202100	380	16	0.098 (121)	0.309 (382)	0.345 (10938)	>99.5	5	16.5±2.0			

Grid reference refers to the *Institut Géographique National* Lambert-IV grid projection; N = number of grains counted; ρ_s = spontaneous track density; ρ_i = induced track density; ρ_d = dosimeter track density; N_s, N_i, N_d = number of tracks counted to determine the reported track densities; $P(\chi^2)$ = Chi-square probability that the single grain ages represent one population; D = age dispersion. All ages are central ages [Galbraith and Laslett, 1993]. Age determinations were performed by BJ except those marked §, which were dated by EL; with ζ = 303±13 (BJ) / 285±3 (EL) for glass dosimeter CN5 and ζ = 342±13 (BJ) / 339±3 (EL) for glass dosimeter NBS962. MTL = Mean horizontal confined Track Length; SD = standard deviation of horizontal confined track length distribution; No Lengths = Number of horizontal confined track lengths measured.

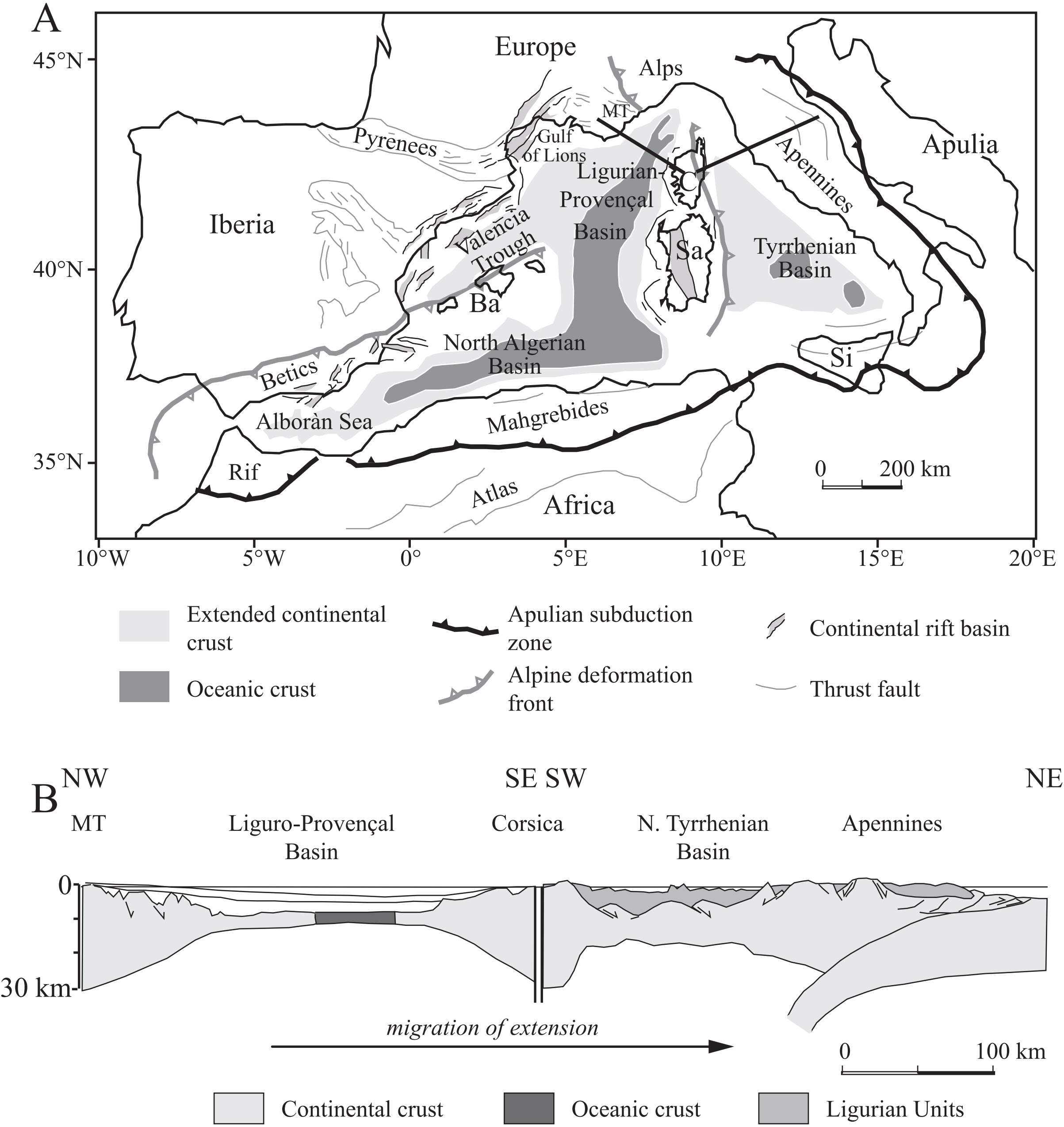

Jakni et al.,
Figure 1

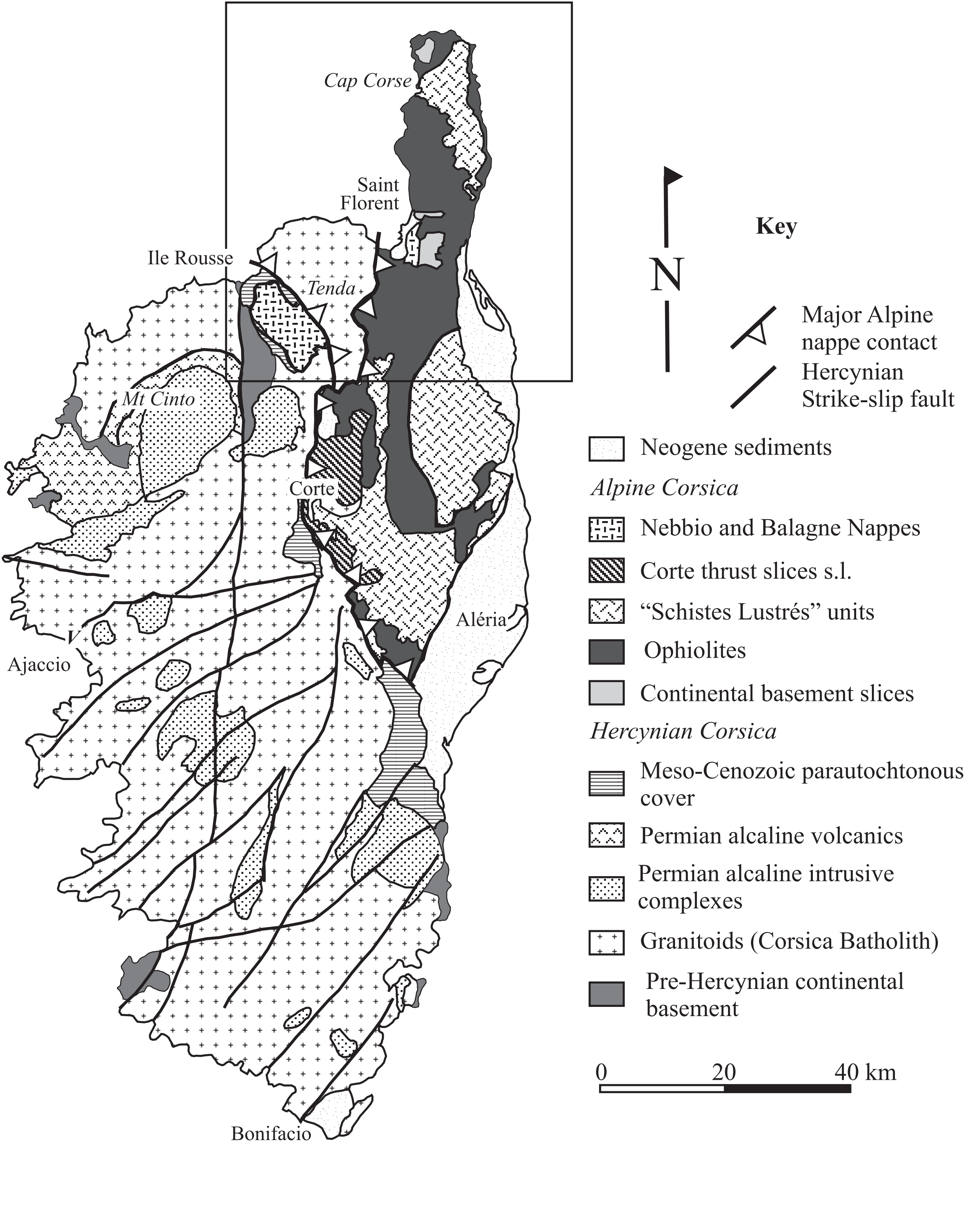

Jakni et al.,
Figure 2

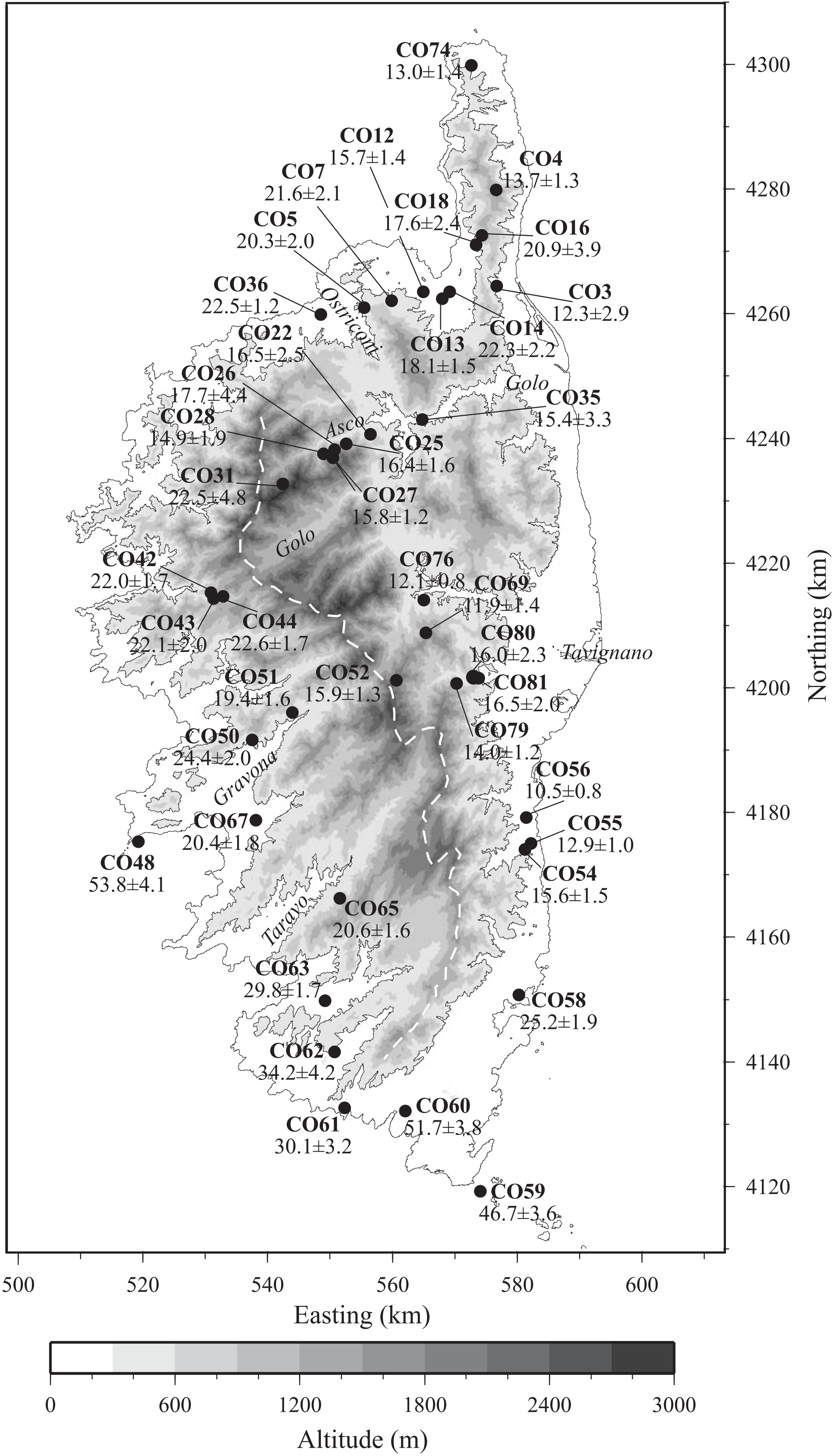
CO74
13.0±1.4
CO12
15.7±1.4
CO4
13.7±1.3
CO7
21.6±2.1
CO18
17.6±2.4
CO5
20.3±2.0
CO16
20.9±3.9
CO36
22.5±1.2
Ostriconi
CO3
12.3±2.9
CO14
22.3±2.2
CO22
16.5±2.5
CO13
18.1±1.5
CO26
17.7±4.4
Golo
CO35
15.4±3.3
CO28
14.9±1.9
Asco
CO25
16.4±1.6
CO31
22.5±4.8
CO27
15.8±1.2
Golo
CO42
22.0±1.7
CO76
12.1±0.8
CO69
11.9±1.4
CO43
22.1±2.0
CO44
22.6±1.7
CO80
16.0±2.3
Tavignano
CO51
19.4±1.6
CO52
15.9±1.3
CO81
16.5±2.0
CO50
24.4±2.0
CO79
14.0±1.2
Gravona
CO56
10.5±0.8
CO67
20.4±1.8
CO55
12.9±1.0
CO48
53.8±4.1
CO54
15.6±1.5
CO65
20.6±1.6
Tarayo
CO63
29.8±1.7
CO58
25.2±1.9
CO62
34.2±4.2
CO60
51.7±3.8
CO61
30.1±3.2
CO59
46.7±3.6
4300
4280
4260
4240
4220
4200
4180
4160
4140
4120
Northing (km)
500
520
540
560
580
600
Easting (km)
0
600
1200
1800
2400
3000
Altitude (m)

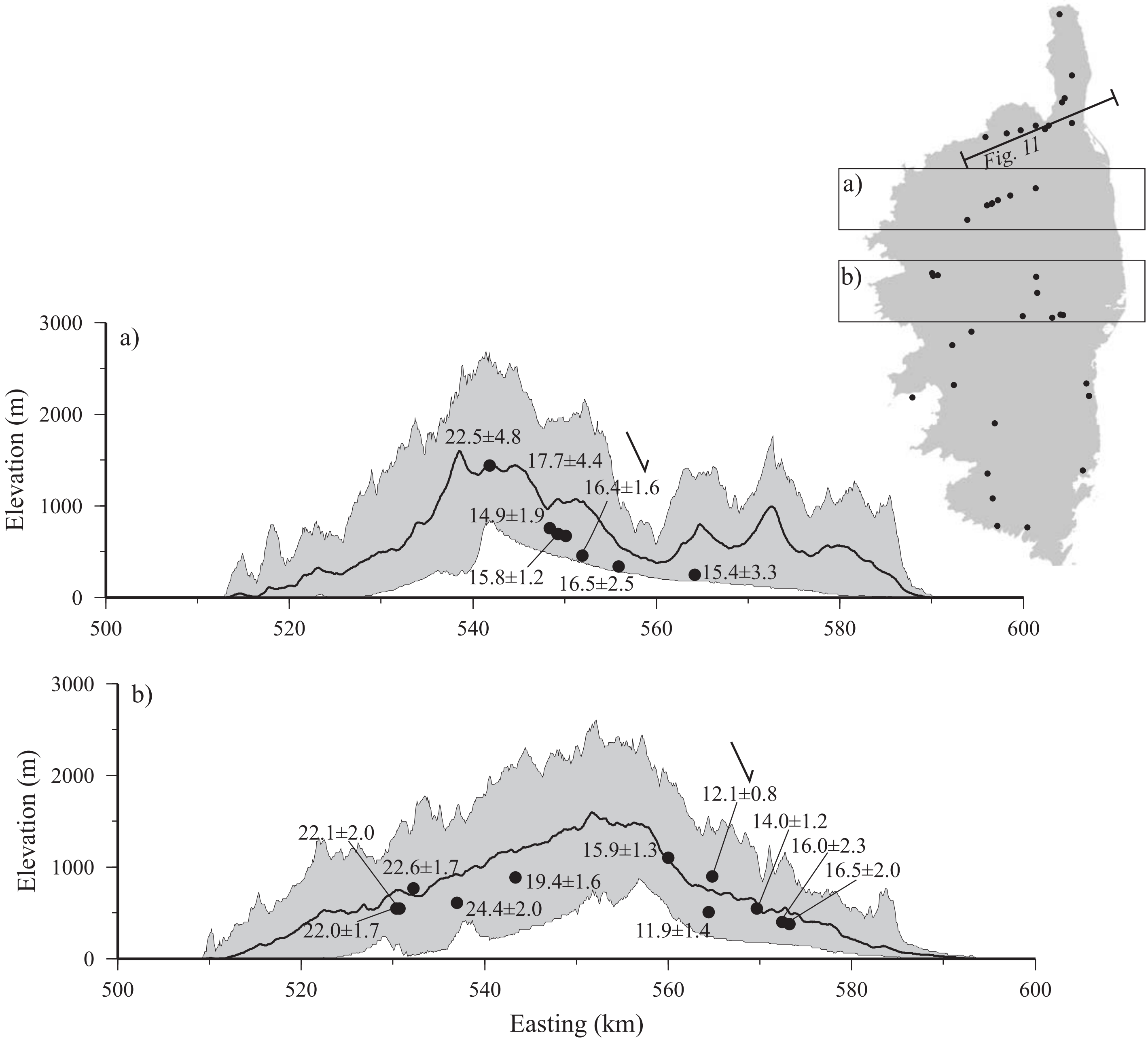

Jakni et al.,
Figure 4

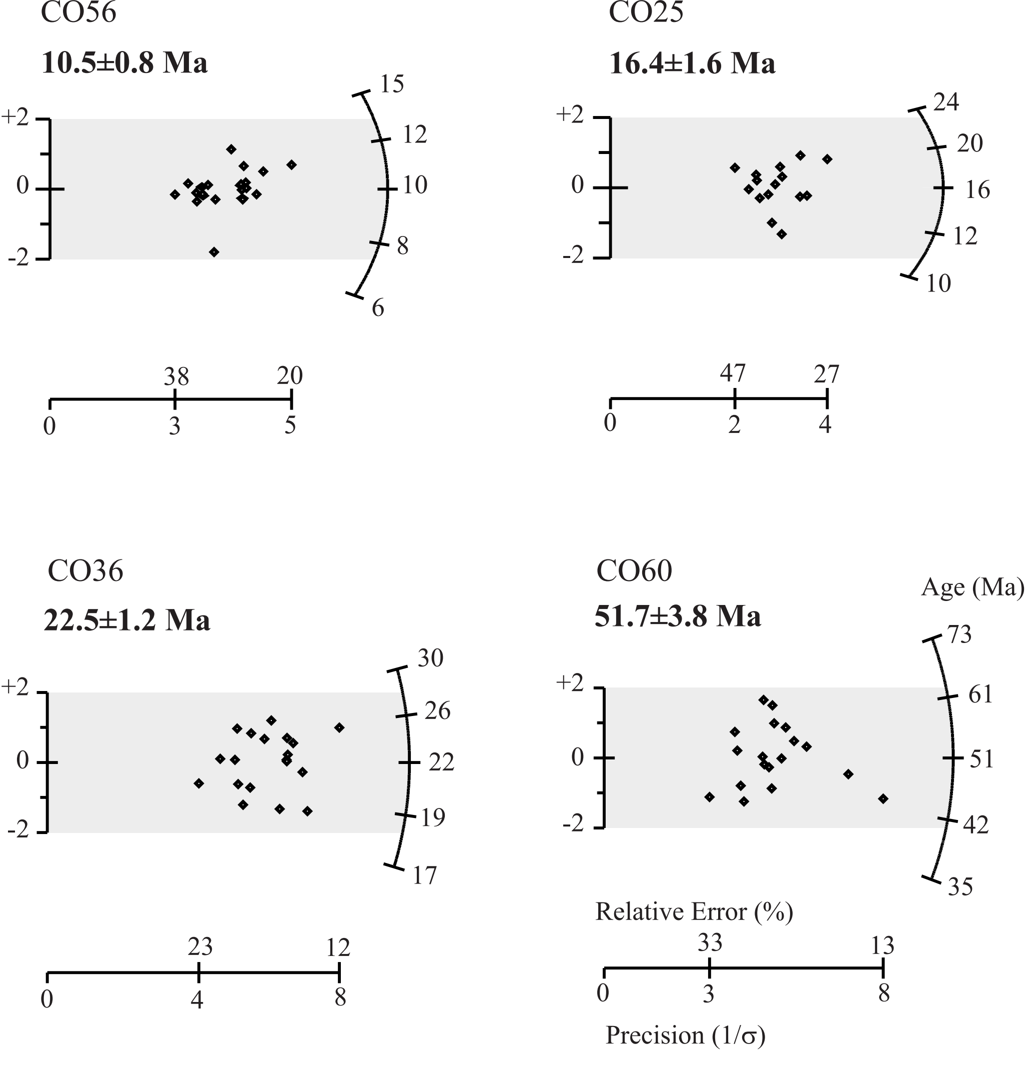

Jakni et al.,
Figure 5

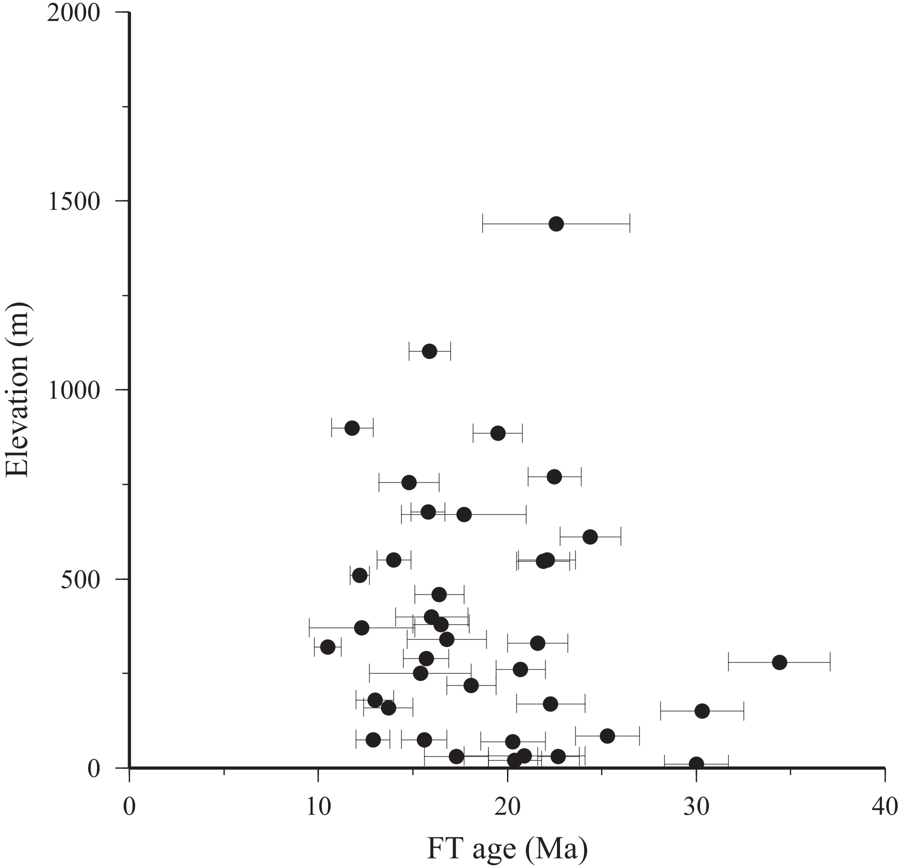

Jakni et al.,
Figure 6

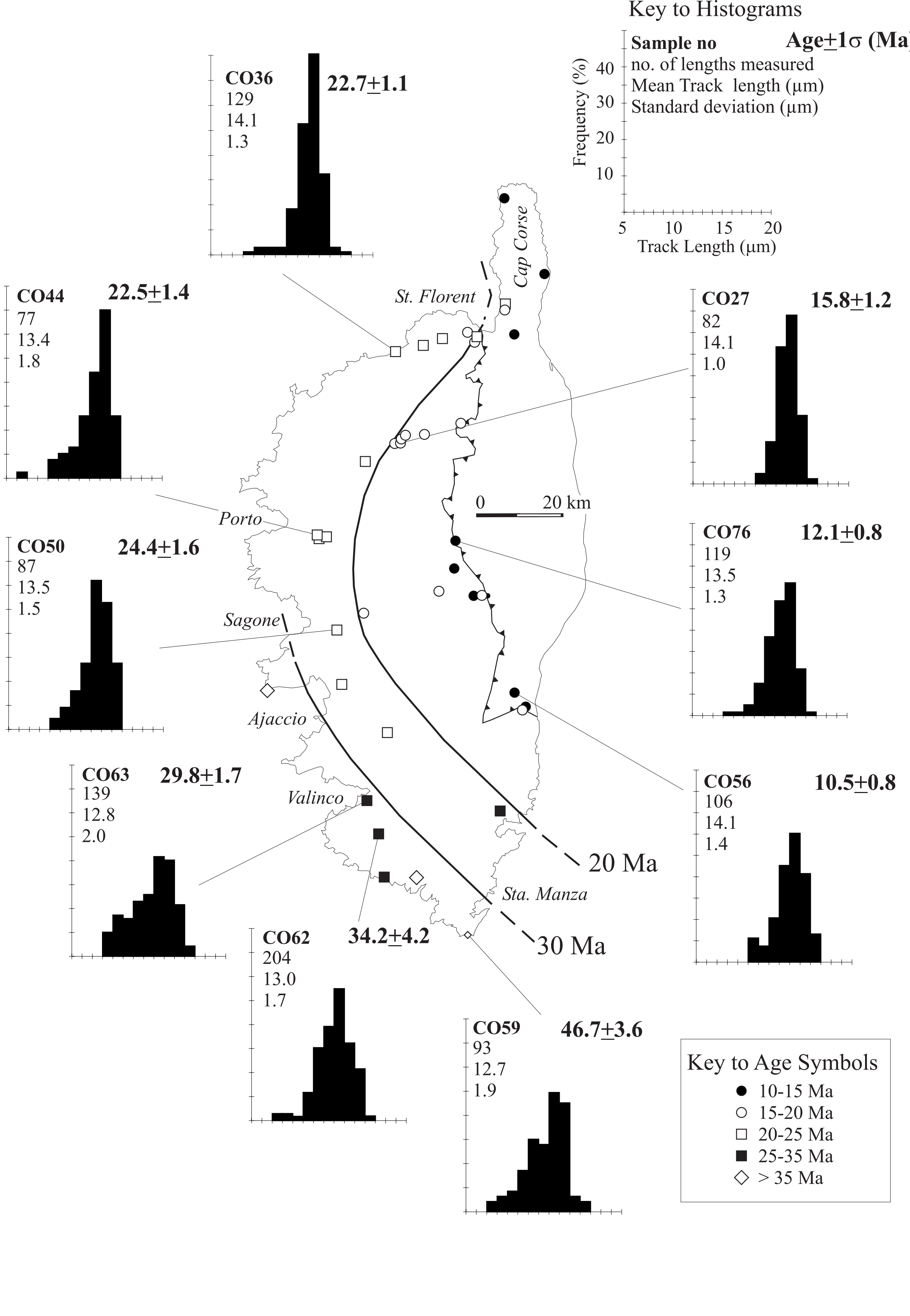

Jakni et al.,
Figure 7

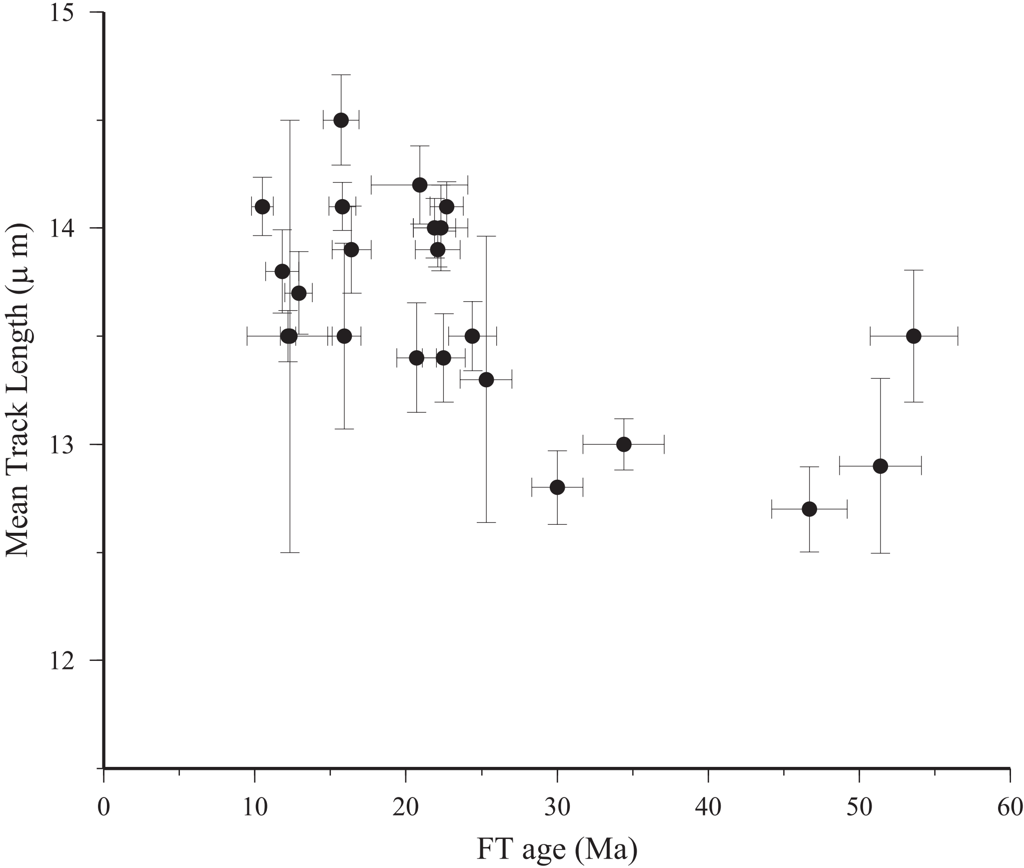

Jakni et al.,
Figure 8

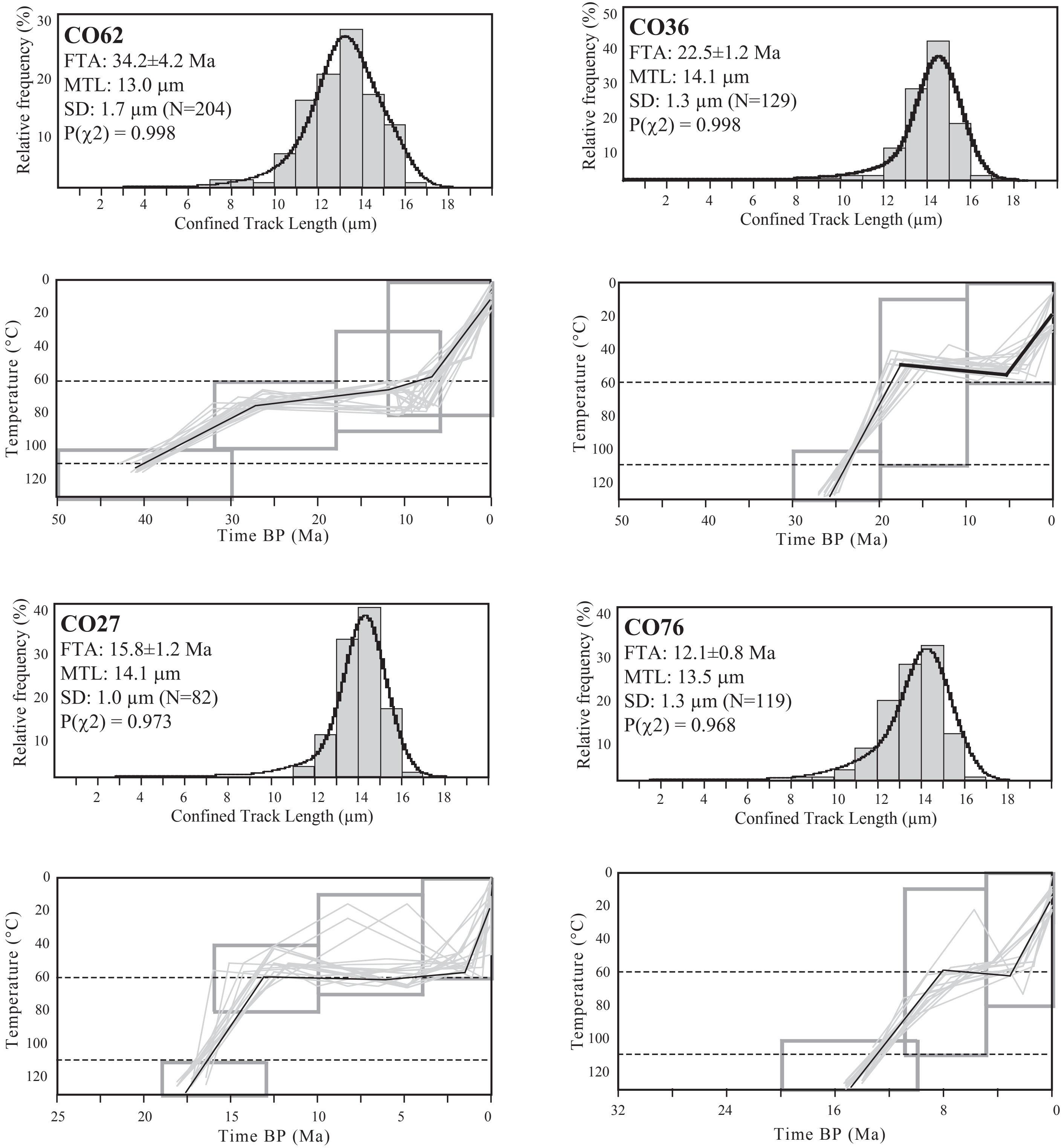

Jakni et al.,
Figure 9

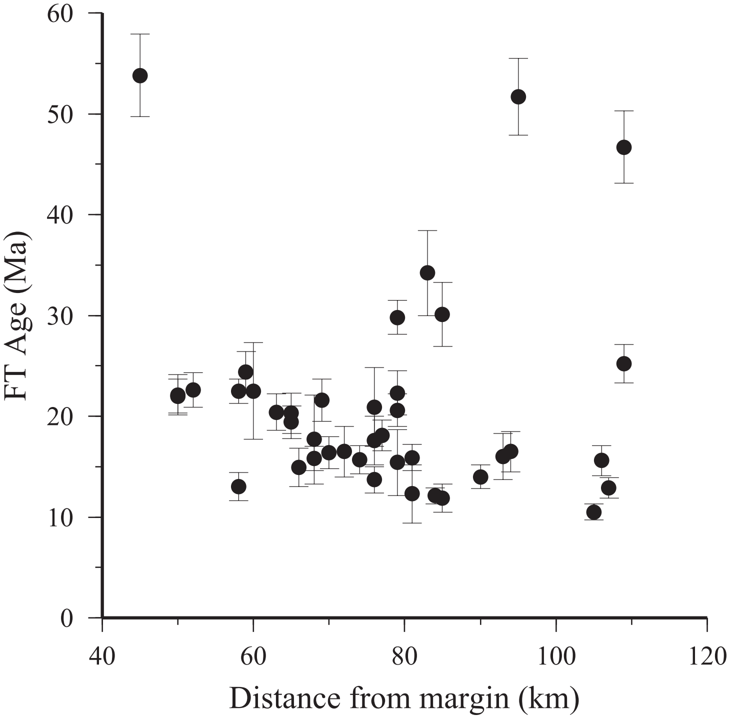

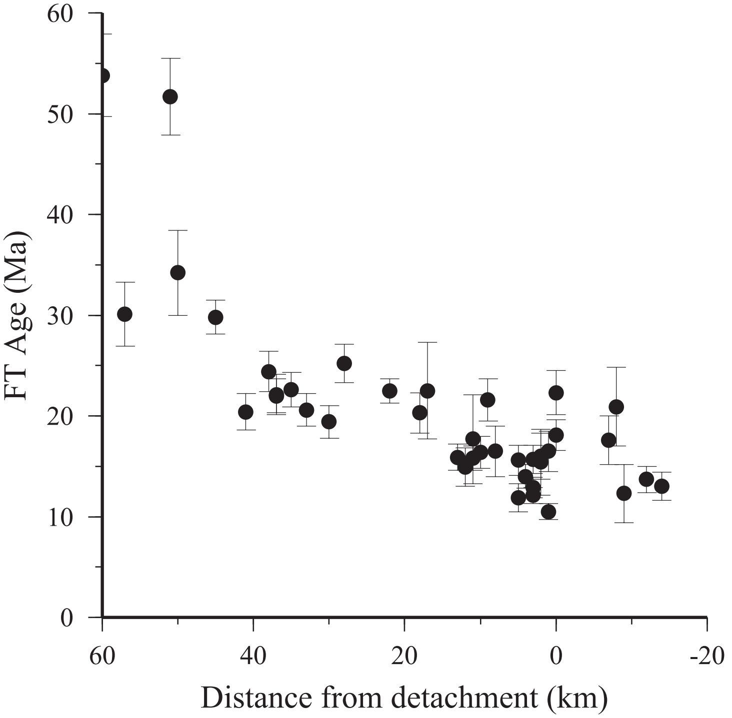

Jakni et al.,
Figure 10

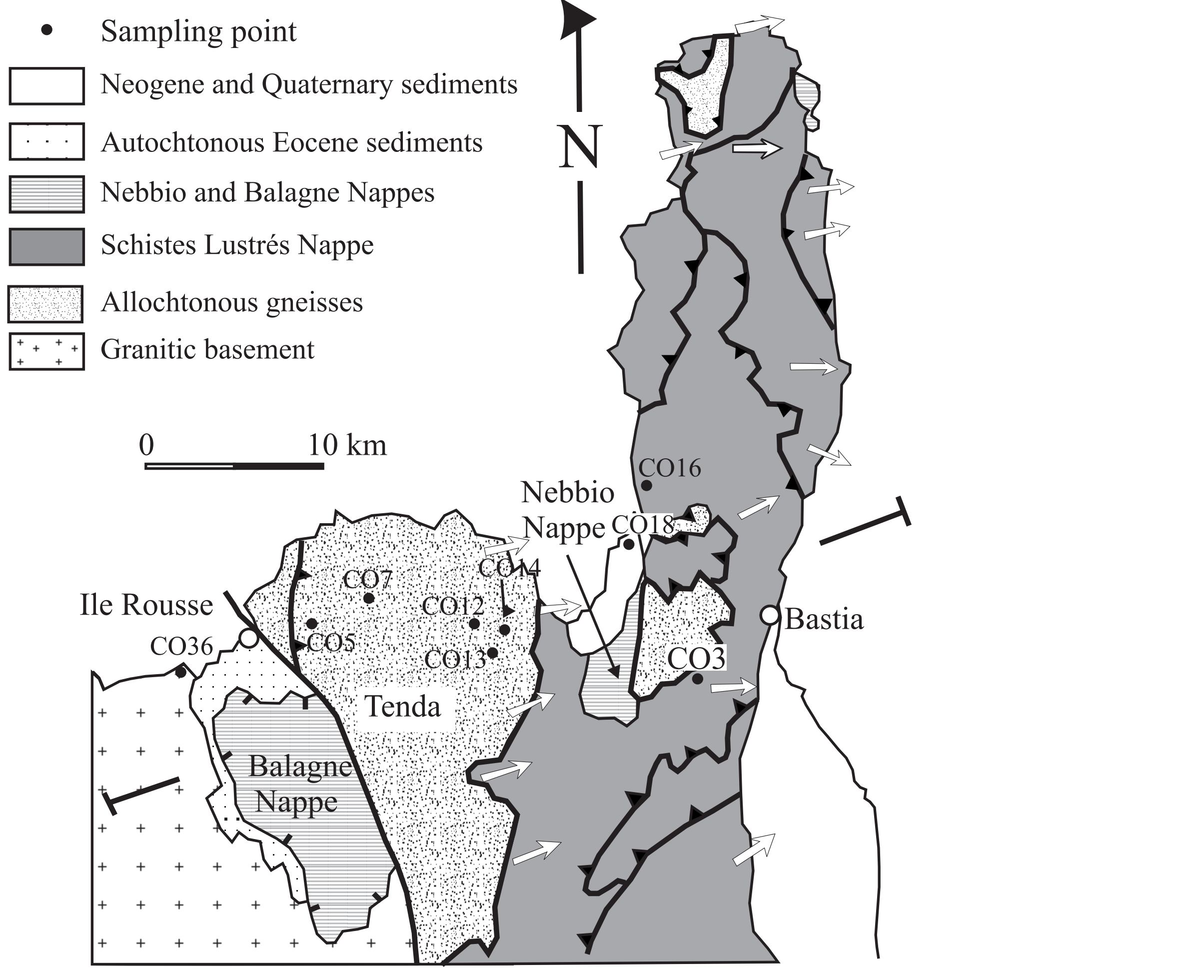
Sampling point
Neogene and Quaternary sediments
Autochtonous Eocene sediments
Nebbio and Balagne Nappes
Schistes Lustrés Nappe
Allochtonous gneisses
Granitic basement
N
0
10 km
CO16
Nebbio
Nappe
CO18
CO14
CO7
CO12
Ile Rousse
CO5
CO36
CO13
CO3
Bastia
Tenda
Balagne
Nappe

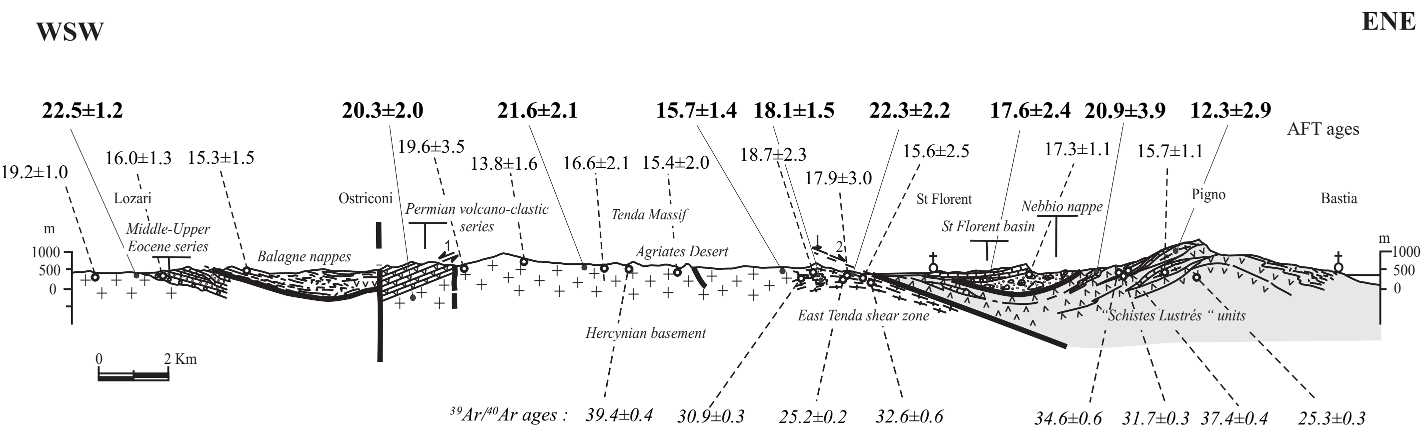
WSW
ENE
22.5±1.2
20.3±2.0
21.6±2.1
15.7±1.4
18.1±1.5
22.3±2.2
17.6±2.4
20.9±3.9
12.3±2.9
AFT ages
19.2±1.0
16.0±1.3
15.3±1.5
19.6±3.5
13.8±1.6
16.6±2.1
15.4±2.0
18.7±2.3
17.9±3.0
15.6±2.5
17.3±1.1
15.7±1.1
Lozari
Middle-Upper
Eocene series
Balagne nappes
Ostriconi
Permian volcano-clastic
series
Tenda Massif
Agriates Desert
St Florent
St Florent basin
Nebbio nappe
Pigno
Bastia
m
1000
500
0
Hercynian basement
East Tenda shear zone
"Schistes Lustrés" units
0
2 Km
$^{39}Ar/^{40}Ar$ ages :
39.4±0.4
30.9±0.3
25.2±0.2
32.6±0.6
34.6±0.6
31.7±0.3
37.4±0.4
25.3±0.3

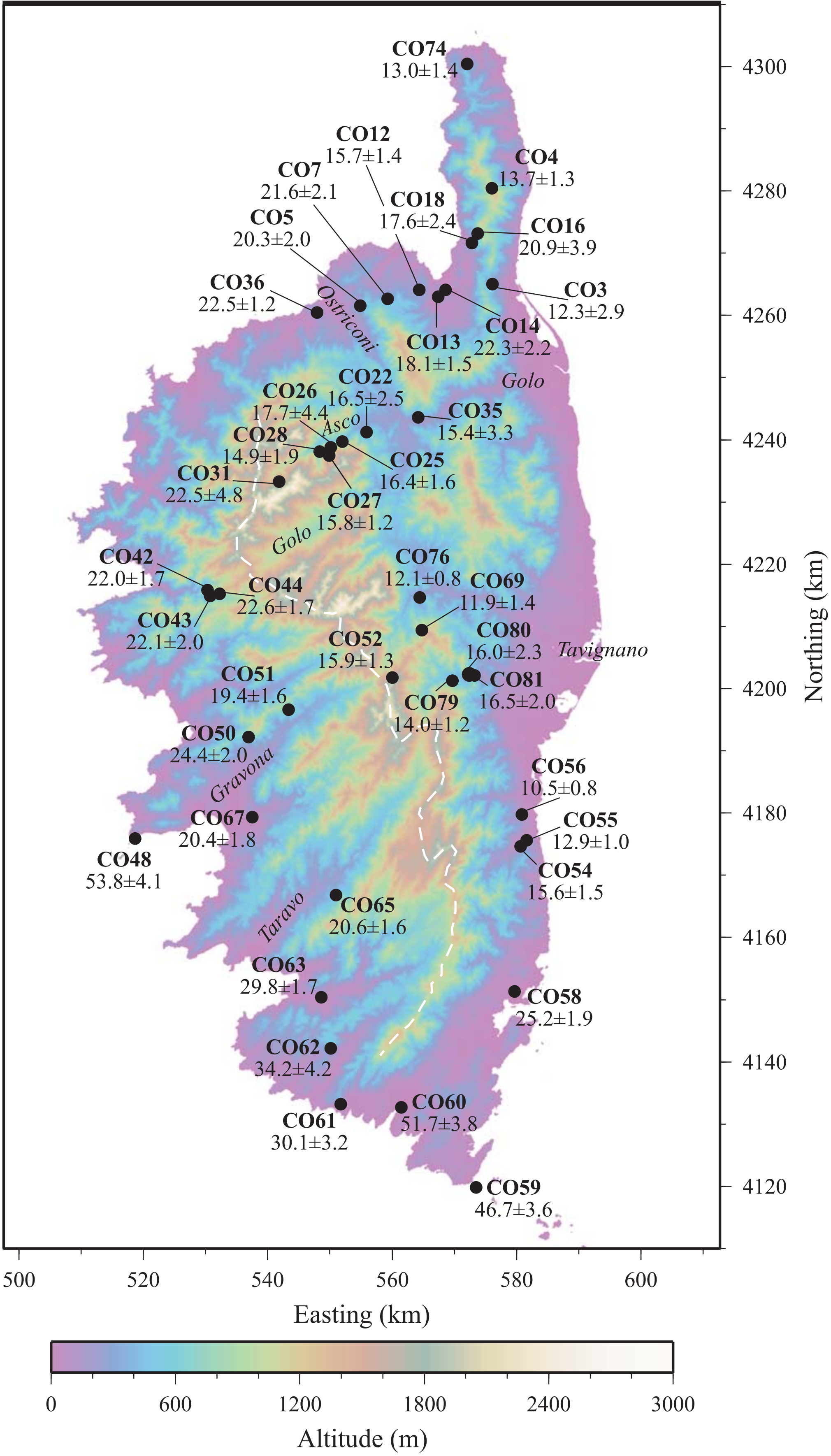

Jakni et al.,
Figure 3